Supplementary Information

Coordination polymer hydrogels through Ag(I)-mediated spontaneous self-assembly of unsubstituted nucleobases and their antimicrobial activity

Bhagwati Sharma, Arup Mahata, Sonam Mandani, Tridib K. Sarma* and Biswarup Pathak*

Discipline of Chemistry, School of Basic Sciences, Indian Institute of Technology Indore, Simrol, Khandwa Road, Indore 452020, India.

Contents

1. Materials and Methods

Materials

Adenine, guanine, cytosine, thymine, uracil and silver perchlorate were purchased from Aldrich chemicals. Silver nitrate was purchased from S. D. Fine chemicals, India. Silver acetate, sodium hydroxide, methanol, acetonitrile, N,N'-Dimethylformamide, potassium bromide, potassium iodide, sodium sulfide and nitric acid were purchased from Merck, India. All the chemicals were of analytical grade and were used without any further purification. Milli Q water was used throughout the experiments.

Instrumentation

Transmission electron microscopy (TEM) images were recorded using a Technai G^2 20 Ultra-Twin microscope at an accelerating voltage of 200 kV. Field emission scanning electron microscopy images were recorded on a Carl Zeiss Supra 55 instrument after coating with gold. Rheological measurements were performed using an Anton Paar Physica MCR 301 rheometer with parallel plate geometry (diameter 50 mm). Powder X-ray diffraction patterns (XRD) of the freeze dried gels were recorded on a Rigaku Smartlab, Automated Multipurpose X-ray diffractometer with Cu Kα source (wavelength of X- rays was 0.154 nm). FTIR spectra were recorded in KBr pellet using Bruker Tensor 27 instrument. Thermogravimetric analysis was performed using a Mettler Toledo thermal analysis system at a heating rate of 5 °C per minute. Solid state UV-visible spectra were recorded on a Perkin Elmer lambda instrument.ICP-MS analysis were performed using a Themo Fischer scientific instrument.

Solubilization of nucleobases in water

Pure nucleobases as such are insoluble in water and a simple chemical modification through deprotonation or protonation using either alkaline or acidic conditions are essential for complete solubilization. Therefore the nucleobases were solubilized in water by the addition of NaOH or HNO_3. The final pH of the solution after complete dissolution of 0.1 M nucleobase in basic medium (through the addition of NaOH) was 10.5, 12.1, 11.0, 10.1 and 9.6 for adenine, guanine, cytosine, thymine and uracil respectively. On the other hand the pH of the solution resulting in complete solubilization in acidic medium was less than 1.0 for all the five nucleobases.

Synthesis of Ag-nucleobase hydrogels in basic medium

Stock solutions of both the nucleobases and $AgNO_3$ were first prepared. A stock solution of each nucleobases (0.1 M) was prepared by the addition of solid NaOH to it in small parts under sonication, until the nucleobase was completely dissolved and a clear solution was obtained. Similarly, $AgNO_3$ solution (0.1 M) was prepared by simple dissolution of the metal salt in water.

In a typical synthesis, 0.8 mL of the as prepared nucleobase solution was taken in a tube and to it 1 mL of the $AgNO_3$ solution was added. The formation of hydrogels was confirmed by visually observing the absence of fluid flow in inverted tube.

Synthesis of Ag-guanine gel in acidic medium

Initially stock solution of guanine (0.1M) was prepared by dissolving the required amount of guanine in water-HNO_3 mixture. In a typical synthesis, 1.0 mL of $AgNO_3$ was added to 1.0 mL of the protonated guanine solution, which resulted in the formation of a hydrogel within a few minutes, as confirmed by inverted tube method.

Electron microscopy studies

The samples for both TEM and FESEM were prepared by diluting the gel samples in water. A small amount of the gel was taken in an eppendorf tube and after addition of water the gel was crushed using a micropestle. The samples were drop casted on a carbon coated copper grid (for TEM) and glass slides (for FESEM), followed by room temperature drying.

Rheological studies

Rheological investigations were performed using parallel plate geometry of diameter 50 mm. For the measurements, the hydrogels were placed on the plate of the rheometer using a microspatula. The temperature was maintained at 25 °C using an integrated temperature controller from Julabo. Dynamic strain sweep experiments were performed using a constant frequency of 10 rad s^{-1}. The dynamic frequency sweep of the hydrogels was measured as function of frequency in the range of 0.1-100 rad s^{-1} with constant strain value 1%.

Study of response of gels towards different anions

The chemical response of the Ag-nucleobase hydrogels was studied by using Ag-thymine gel as the model gel. The gel was first prepared by adding 0.75 mL of $AgNO_3$ (0.2 M) to 0.6 mL of deprotonated thymine (0.2 M). To the gels taken in different tubes, 0.15 mL of 1.0 M KBr, KI and Na_2S was added and allowed to stand for 12 hours, upon which the gel was converted to sol with precipitates. The precipitate was then removed by centrifugation. On addition of 0.75 mL of $AgNO_3$ (0.1 M) solution to the supernatant, spontaneous formation of the gel was observed.

Antimicrobial studies

The antimicrobial activity of the hydrogels was studied using the cup-plate method. Initially, both the gram negative *E. Coli* and the gram positive *S. aureus* were cultured in the nutrient broth by incubation at 37 °C for 24 hours. Then nutrient media was prepared and inoculated with 1 ml of suitable suspension of the bacteria which was then poured in a petri-dish and allowed to cool to room temperature, upon which the agar solidified. Four holes were cut in the agar by means of a 10 mm cork borer in which the gels to be tested were filled. The petri dish was then incubated at 37 °C for 24 hours, and the zone of inhibition was measured.

Study of release of silver

The release of silver from the hydrogels was carried out in PBS solution. Briefly 1g of the hydrogels was immersed in 20 mL of PBS for a time period of one and six hours. The concentration of silver was determined using inductively coupled plasma method after filtration.

DFT Calculations

DFT calculations were performed using M06-2X level of theory as implemented in Gaussian 09 program[1]. This functional was considered for our calculations as the dispersion interaction is more accurately defined for non-bonded interactions[2]. 6-311++G** basis set was used for the main group atoms and DGDZVP for the silver atoms. The effects of the water hydration on the structures and relative energy of complexes were taken into account by means of the polarizable continuum model (PCM)[3-6]. The gas phase structures were re-optimized within the PCM. Binding energies were calculated as the difference between the electronic energy of the complexes and the respective monomers, i.e.

$\Delta E = E_{N-Ag} - (E_N + E_{Ag})$,

Where $E_{N\text{-}Ag}$ is the total energy of the nucleobase-silver complex, E_N and E_{Ag} are the energies of the nucleobases and silver ion respectively.

Supplementary Figures for Ag-adenine hydrogels

Figure S1. Digital image of the Ag-adenine hydrogel showing the absence of flow upon inversion.

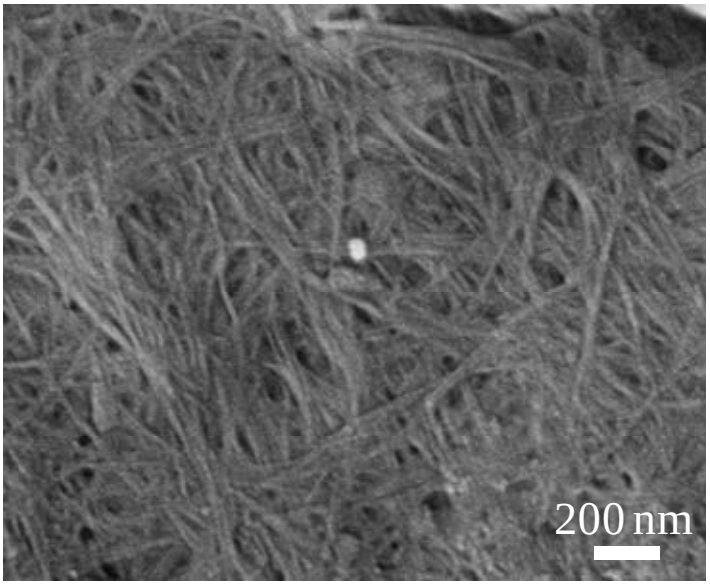

Figure S2. Self-assembled structure at low concentration: FESEM image of fibrous structures from a turbid solution formed upon the addition of 10 mM $AgNO_3$ solution to an alkaline solution of adenine (10 mM), maintaining a metal:adenine ratio of 1:0.8.

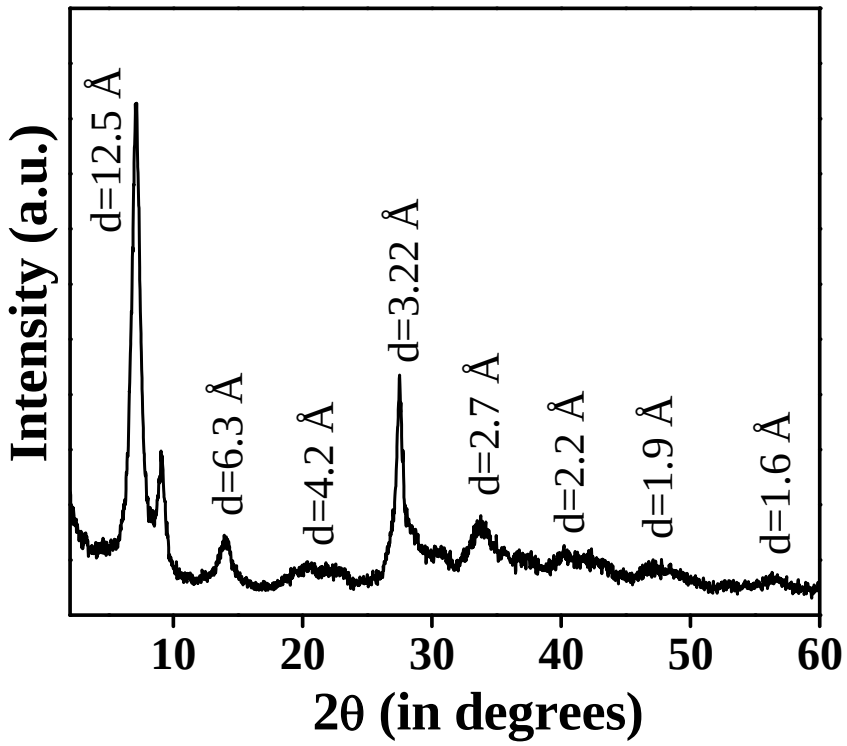

Figure S3. Powder XRD pattern of the lyophilized Ag-adenine hydrogel showing well resolved diffraction peaks.

The wide angle X-ray diffraction pattern of the lyophilized Ag-adenine hydrogels deposited on a glass plate were all characterized by a group of well-resolved reflections, suggesting that the hydrogel was highly crystalline in nature. Major diffraction peaks at 2θ = 7.1°, 14.1°, 21.2°, 27.5°, 33.8°, 42.1°, 47.2° and 56.2° with corresponding d-values of 12.5 Å, 6.3 Å, 4.2 Å, 3.2 Å, 2.1 Å, 1.7 Å, 1.5 Å and 1.3 Å respectively were observed. These peaks followed a ratio of 1: 1/2: 1/3: 1/4: 1/5: 1/6: 1/7: 1/8, suggesting that the hydrogels were mainly assembled in a layered structure with the interlayer distance of 12.5 Å.

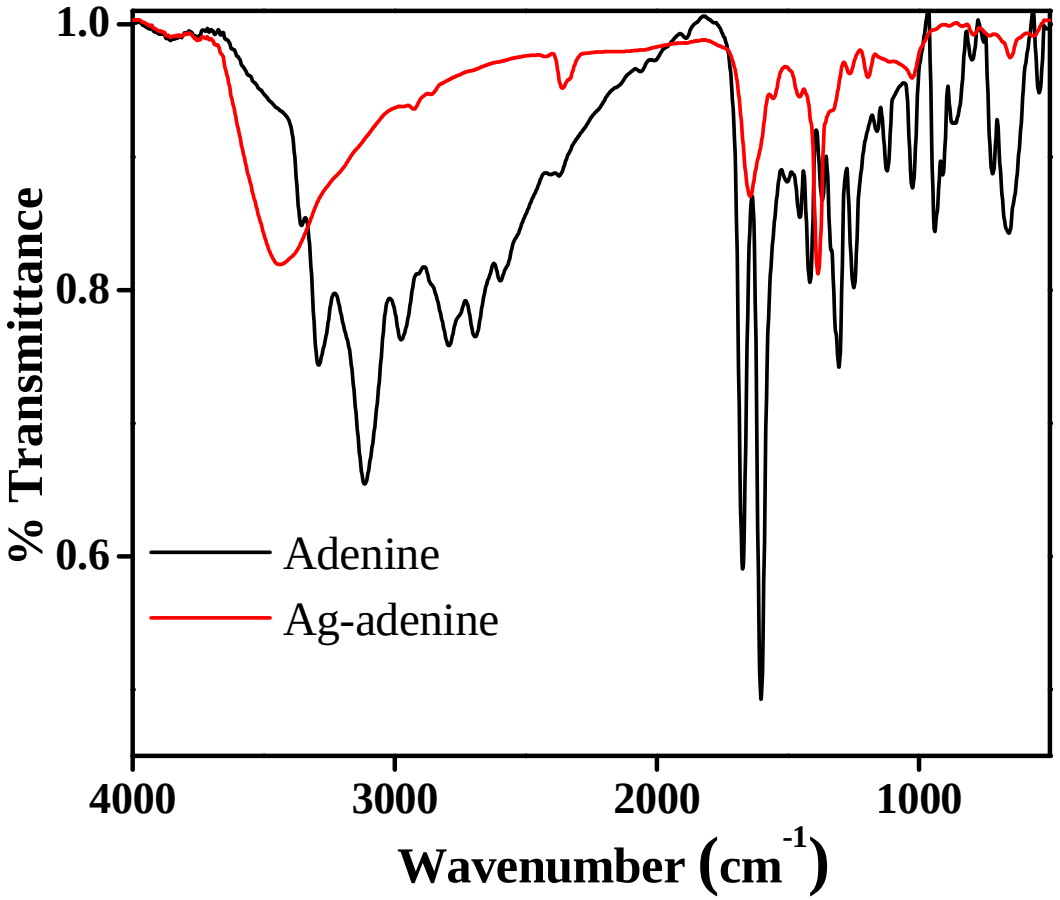

Figure S4. FTIR spectrum of pure adenine and freeze dried Ag-adenine hydrogel.

From the FTIR spectrum of pure adenine and Ag-adenine hydrogel it was observed that the peaks at 3310 cm^{-1} and 3110 cm^{-1} due to NH_2 stretching in pure adenine disappeared in the complex and a new broad peak at 3440 cm^{-1} was observed due to O-H stretching vibrations, which might have arisen due to the trapped water molecules. Further the peak at 2790 cm^{-1} due to N-H stretching in adenine disappeared in the complex, suggesting the probable involvement of N9 of adenine in metal coordination. Again, the peak at 1670 cm^{-1} in pure adenine, which is observed due to NH_2 scissoring, shifted to 1642 cm^{-1} in the Ag-adenine complex, indicating the probable involvement of NH_2 in binding to silver ions or in H-bonding. The peak at 1259 cm^{-1} due to N-H bending in adenine disappeared in the complex, again indicating the involvement of N9 in coordination to Ag^+ ions.

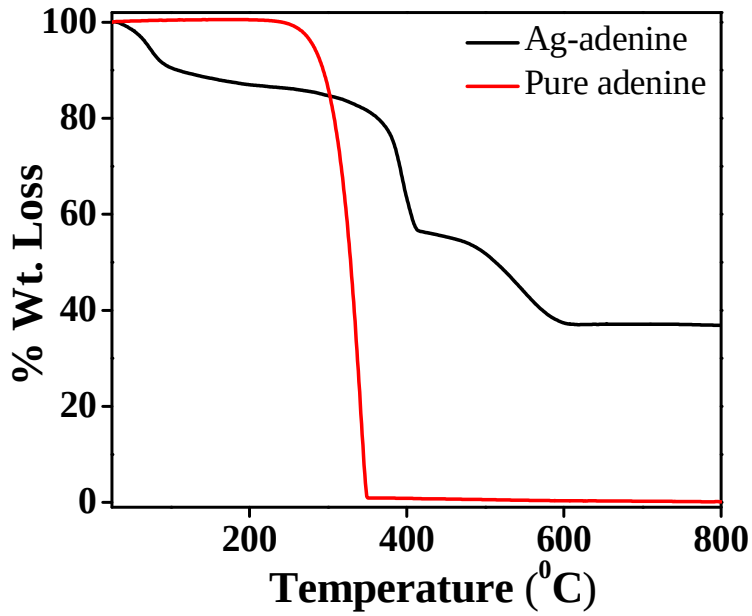

Figure S5. Thermogravimetric analysis plot for pure adenine and Ag-adenine gel.

Thermogravimetric analysis of the freeze dried gel was performed to have an idea about the thermal stability of pure adenine and Ag-adenine gel. The TGA plot for pure adenine showed a single weight loss in the temperature range of 275 °C-350 °C , whereas for the Ag-A xerogels, initial weight loss of approx. 10% at a temperature of 102 °C, which is assumed to be due to the loss of water molecules in the hydrogel matrix was observed. No significant weight loss was observed thereafter upto a temperature of 340 °C. Further, two weight losses at 340 °C and 450 °C were observed which can be attributed to the decomposition of the ligand (adenine). The residual material (37%), which is assumed to be the metallic component, was thereafter stable upto a temperature of 800 °C.

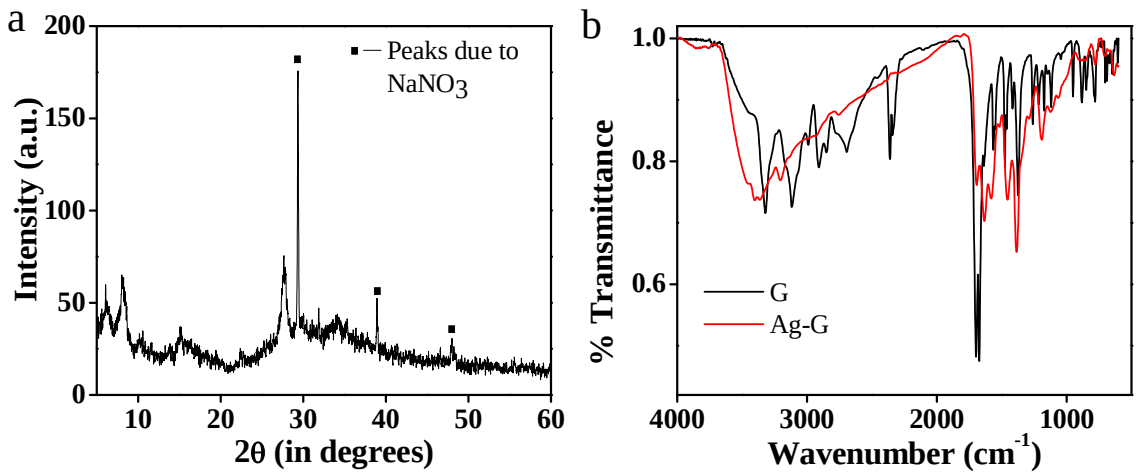

Figure S6. (a) Powder XRD pattern of the Ag-guanine precipitate in alkaline medium and (b) FTIR spectrum of pure guanine and Ag-guanine precipitate in basic medium.

Powder X-ray diffraction of the dried Ag-guanine precipitate showed crystallinity of the composite with major peaks arising at 2θ = 6.0°, 8.2°, 10.4°, 15.2°, 27.7° and 34.1° along with several sharp peaks originating from $NaNO_3$ (figure S6a). The most intense peak at 2θ = 27.7° corresponds to *d*-value of 3.2 Å, which is very close to that of π-π stacking interactions in guanine based hydrogels[7]. From the FTIR spectrum (figure S6b), it was observed that the medium intensity, sharp peak at 2695 cm^{-1} in case of pure guanine disappeared after addition of Ag^+ ions suggesting the probable involvement of N9 or N1 of guanine in binding to Ag^+. Again the shoulder peak at 2990 cm^{-1} in pure guanine arising due to N-H stretching of amide was absent in the complex, indicating that the N1 position of guanine was engaged in binding to Ag^+. Further, the peak at 1698 cm^{-1} in case of pure guanine due to C=O stretching vibrations shifted to 1691 cm^{-1} in the complex, suggesting the probable involvement of oxygen in H-bonding. The involvement of N1 or N9 positions in binding to Ag^+ ions was further supported by the absence of the peak at 1259 cm^{-1} due to N-H bending vibrations in the Ag-guanine complex.

Ag^+	Adenine	Result
1	0.8	Gel
1	1	Gel with some water
2	1	Gel
0.25	1	Partial gel formation, with the gel floating in the excess nucleobase solution

Table S1. Supramolecular structure formed by the interaction of Ag^+ ions and adenine at various Ag^+:adenine molar ratio.

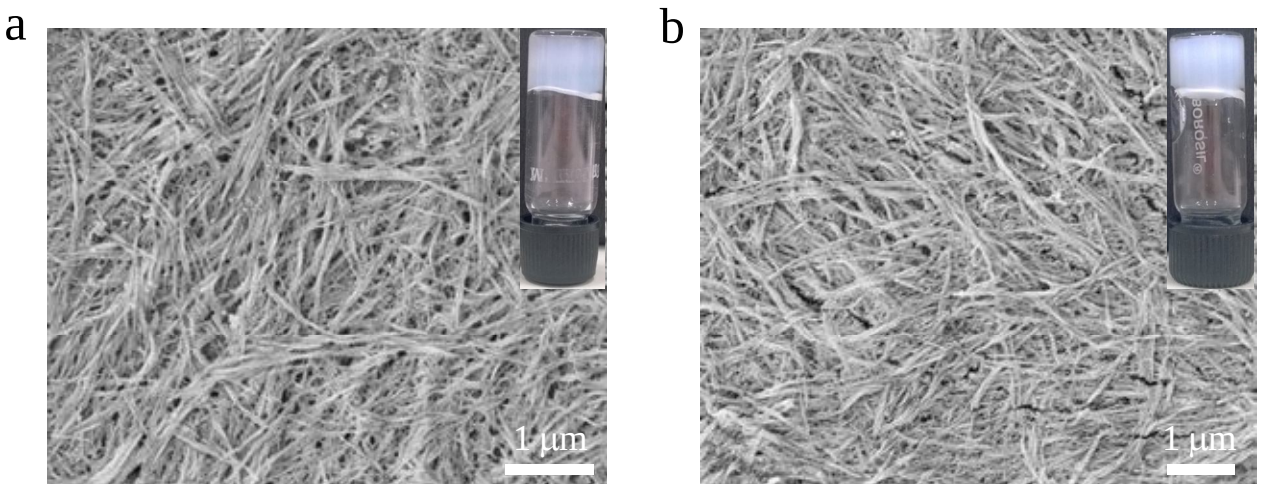

Figure S7. FESEM images of Ag-adenine hydrogel formed using alkaline adenine and (a) CH_3COOAg and (b) $AgClO_4$. *Inset:* Digital images of the respective hydrogels.

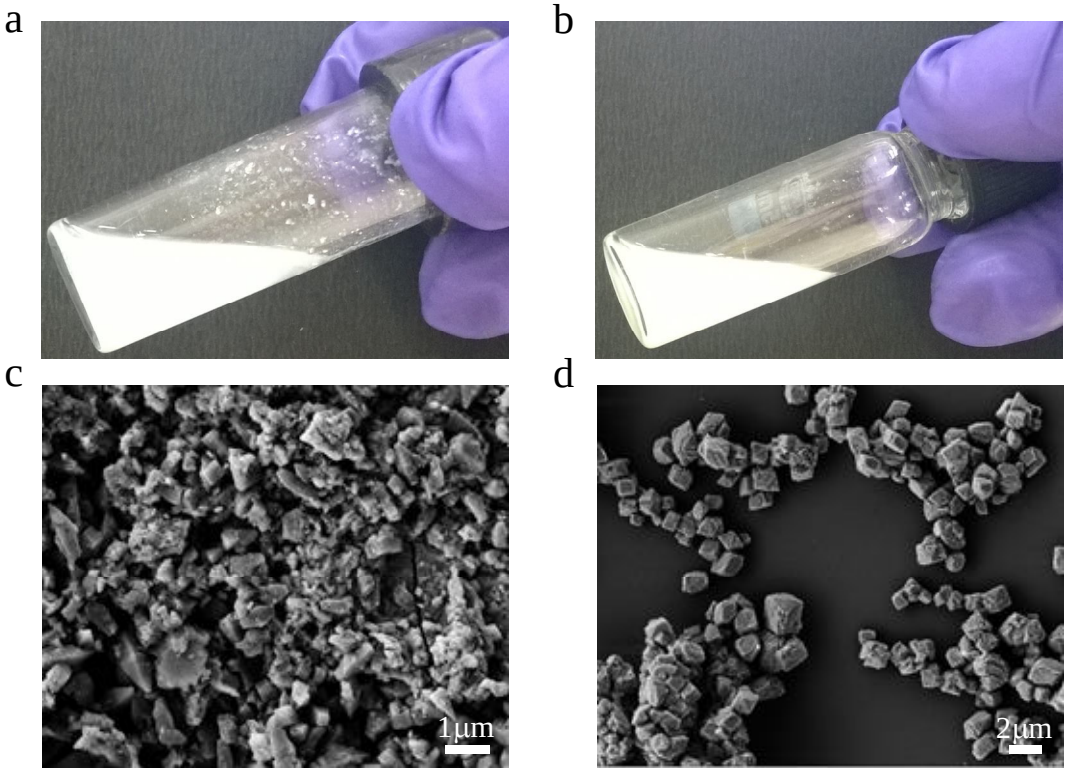

Figure S8. (a) and (b) Digital images of Ag-adenine precipitate formed in methanol and DMF as solvents respectively. (c) and (d) are FESEM images of the precipitates obtained upon the addition of Ag^+ ions to alkaline adenine solution in methanol and in DMF respectively.

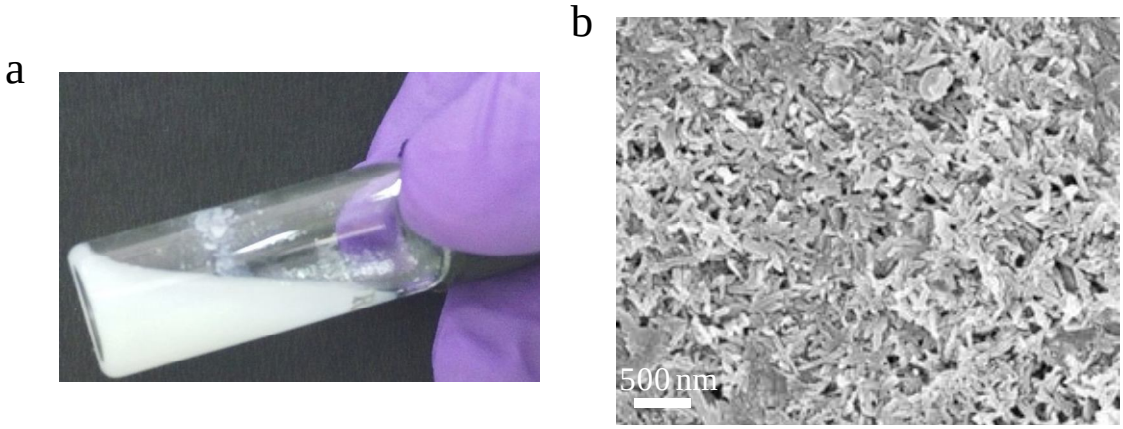

Figure S9. (a) Digital image of the precipitate obtained upon the addition of a methanolic solution of $AgNO_3$ to an alkaline DMF solution of adenine. (b) FESEM image of the Ag-adenine precipitate formed in MeOH-DMF mixture solvent system.

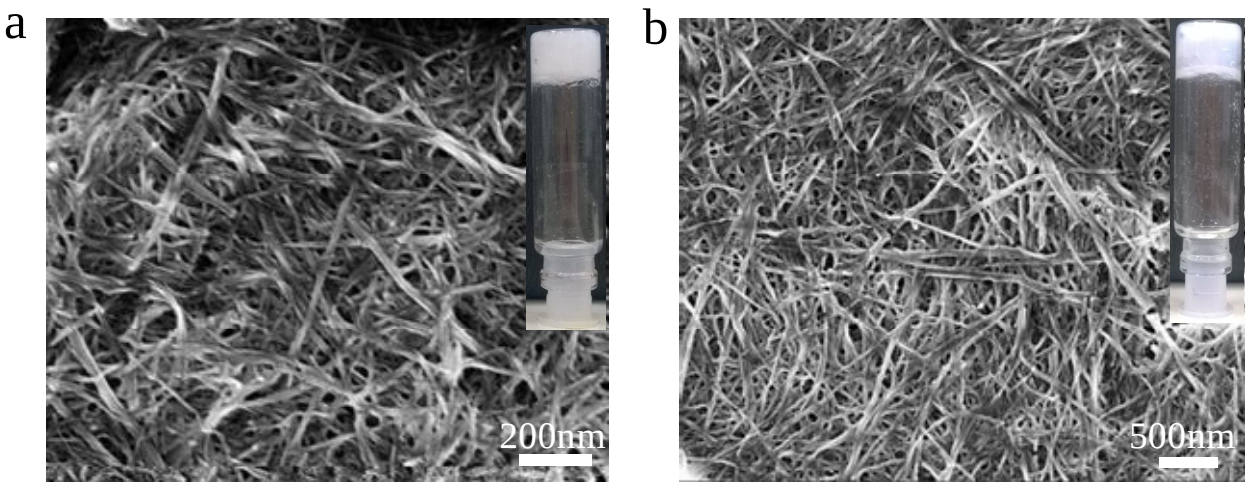

Figure S10. FESEM images of the Ag-adenine gels formed in (a) methanol-H_2O mixture and (b) acetonitrile-H_2O mixture; *inset*: Digital images of the respective hydrogels.

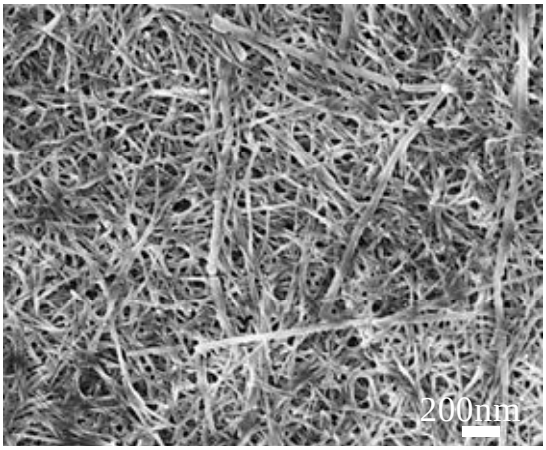

Figure S11. FESEM image of the partial gel formed upon the addition of Ag^+ ions in DMF to an alkaline solution of adenine (in water).

Entry	Solvent system	Result
1	CH_3OH	Precipitate
2	DMF	Precipitate
3	CH_3OH-H_2O	Gel
4	DMF-H_2O	Partial gel formation
5	CH_3CN-H_2O	Gel
6	CH_3OH-DMF	Precipitate

Table S2. Gelation studies of Ag-adenine gel in different solvents and mixed solvent systems

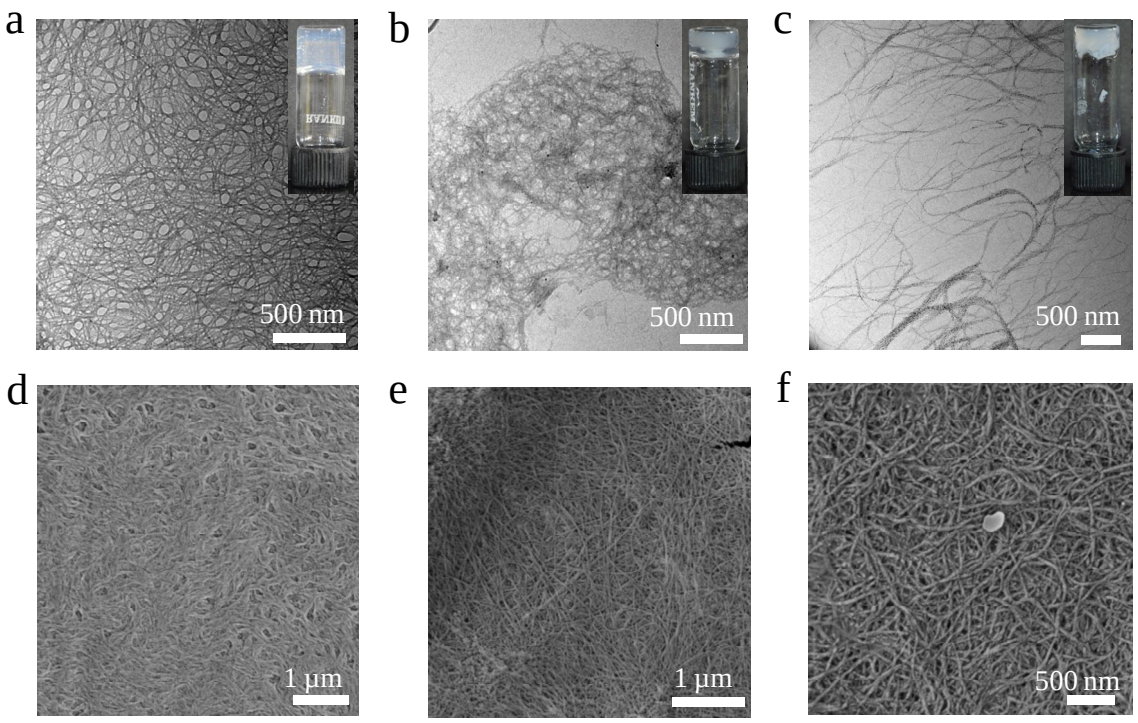

Figure S12. (a), (b) and (c) TEM images of Ag-C, Ag-T and Ag-U hydrogels respectively; *Inset*: Digital image of the respective hydrogels. (d), (e) and (f) FESEM images of Ag-C, Ag-T and Ag-U hydrogels respectively.

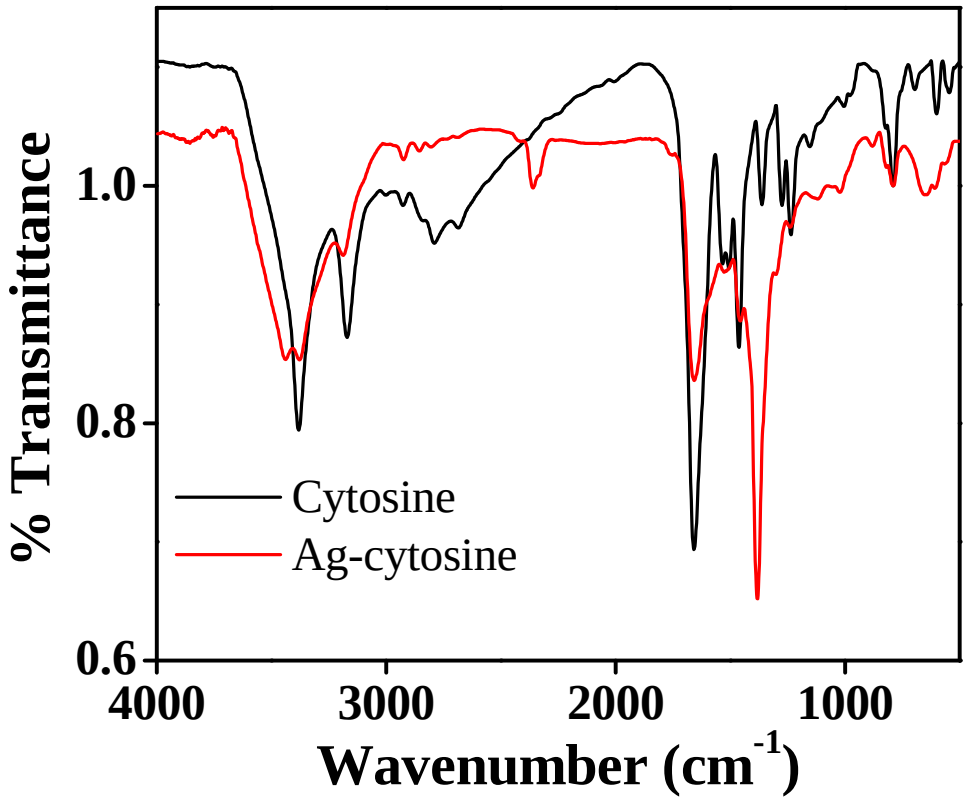

Figure S13. FTIR spectrum of pure cytosine and freeze dried Ag-cytosine hydrogel.

In the FTIR spectrum of pure cytosine and the Ag-cytosine complex, it was observed that the intense peaks at 3380 cm^{-1} and 3160 cm^{-1} due to NH_2 stretching vibrations in pure cytosine decreased in intensity, upon the coordination to Ag^+, probably due to their involvement in H-bonding. Again the weak peak at 2780 cm^{-1} due to N-H stretching was absent in the complex, suggesting the involvement of the N1 nitrogen of cytosine in bonding to the Ag^+ ions. The binding of N1 to silver was further supported by the loss of the peak at 1270 cm^{-1} due to N-H bending vibrations in the complex.

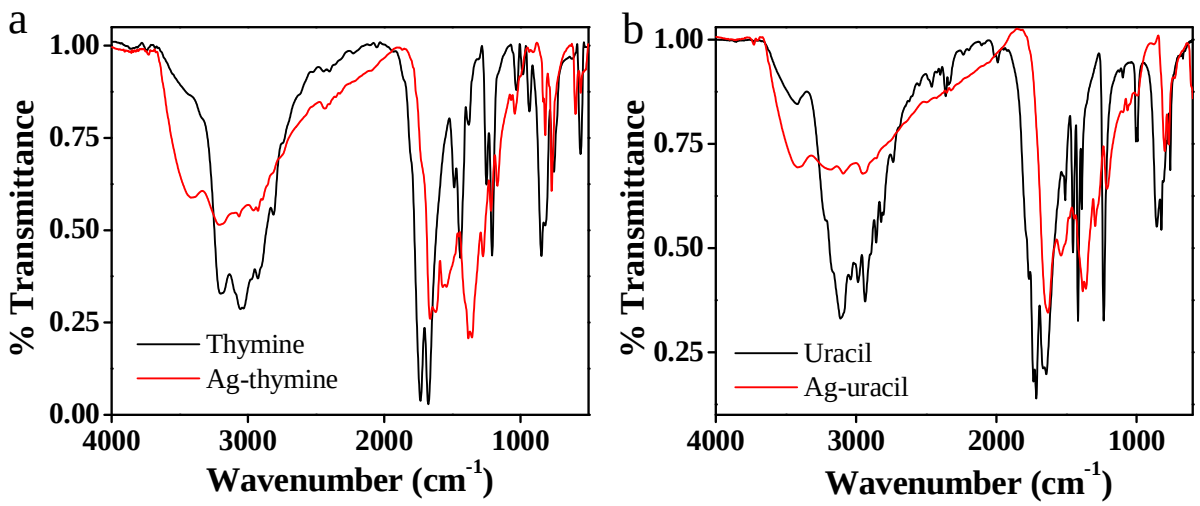

Figure S14. FTIR spectrum of (a) pure thymine and freeze dried Ag-thymine hydrogel and (b) pure uracil and Ag-uracil hydrogel.

For the Ag-thymine gel (Fig. S14a), the weak peak at 2805 cm^{-1} due to N-H stretching in thymine disappeared, suggesting the engagement of the N1 or N3 sites in metal binding. Further, it was observed that the peak at 1730 cm^{-1} due to C=O stretching vibrations shifted to 1660 cm^{-1}, suggesting that the oxygen atoms are also involved in binding to Ag^{+} ions or in H-bonding. Again the disappearance of the peak at 1250 cm^{-1} due to N-H bending was a signature of the binding of Ag^{+} ions to either N1 or N3 position of thymine.

Similarly, for the Ag-uracil gel (Fig. S14b), the peak at 2815 cm^{-1} in pure uracil due to N-H stretching disappeared in complex, signifying the binding of metal to either the N1 or N3 site. Also the peak at 1720 cm^{-1} due to C=O stretching was shifted to 1640 cm^{-1}, suggesting its probable involvement in binding to Ag^{+} ions. Further, the peak at 1240 cm^{-1} in pure uracil due to N-H bending was absent in the complex, thus confirming the binding of Ag^{+} ions to the N1 or N3 site of uracil.

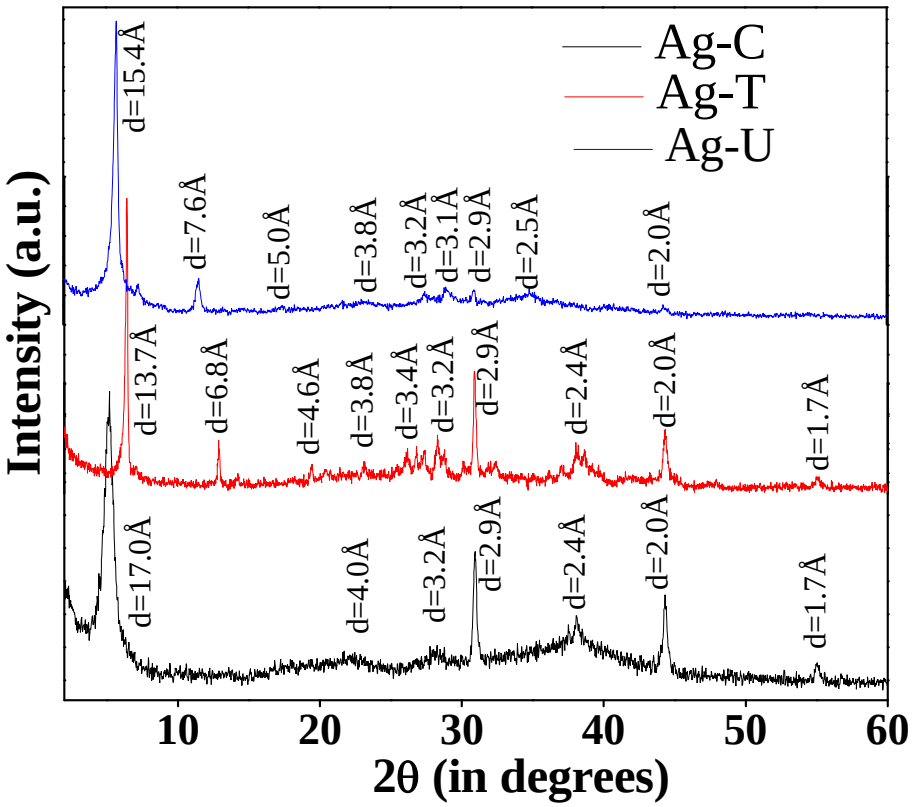

Figure S15. Powder XRD pattern of the lyophilized Ag-cytosine (black), Ag-thymine (red) and Ag-uracil (blue) hydrogels.

The crystalline nature of the nanofibers formed in the three hydrogels was confirmed from the powder XRD studies, which showed several peaks in the 2θ range of 1-60 degrees. For the Ag-thymine gel, well resolved diffraction peaks at 2θ = 6.5°, 12.9°, 19.4°, 23.1° and 30.8° corresponding to a *d*-spacing of 13.7 Å, 6.9 Å, 4.6 Å, 3.8 Å and 2.9 Å respectively were observed. For the Ag-uracil gel, well-resolved diffraction peaks 2θ = 5.7°, 11.6°, 17.5°, 23.2° and 27.5° corresponding to a *d*-spacing of 15.4 Å, 7.6 Å, 5.0 Å, 3.8 Å and 3.2 Å respectively were observed in addition to several other peaks. For both the Ag-thymine and Ag-uracil gels, the peaks followed a periodic ratio of 1: 1/2: 1/3: 1/4: 1/5, similar to the Ag-adenine gel, which suggested that the hydrogels were arranged in a layered structure with an interlayer separation of 13.7 Å and 15.4 Å respectively. On the other hand, for the Ag-cytosine hydrogel, although well-resolved diffraction peaks could be seen, such periodic reflections were not observed.

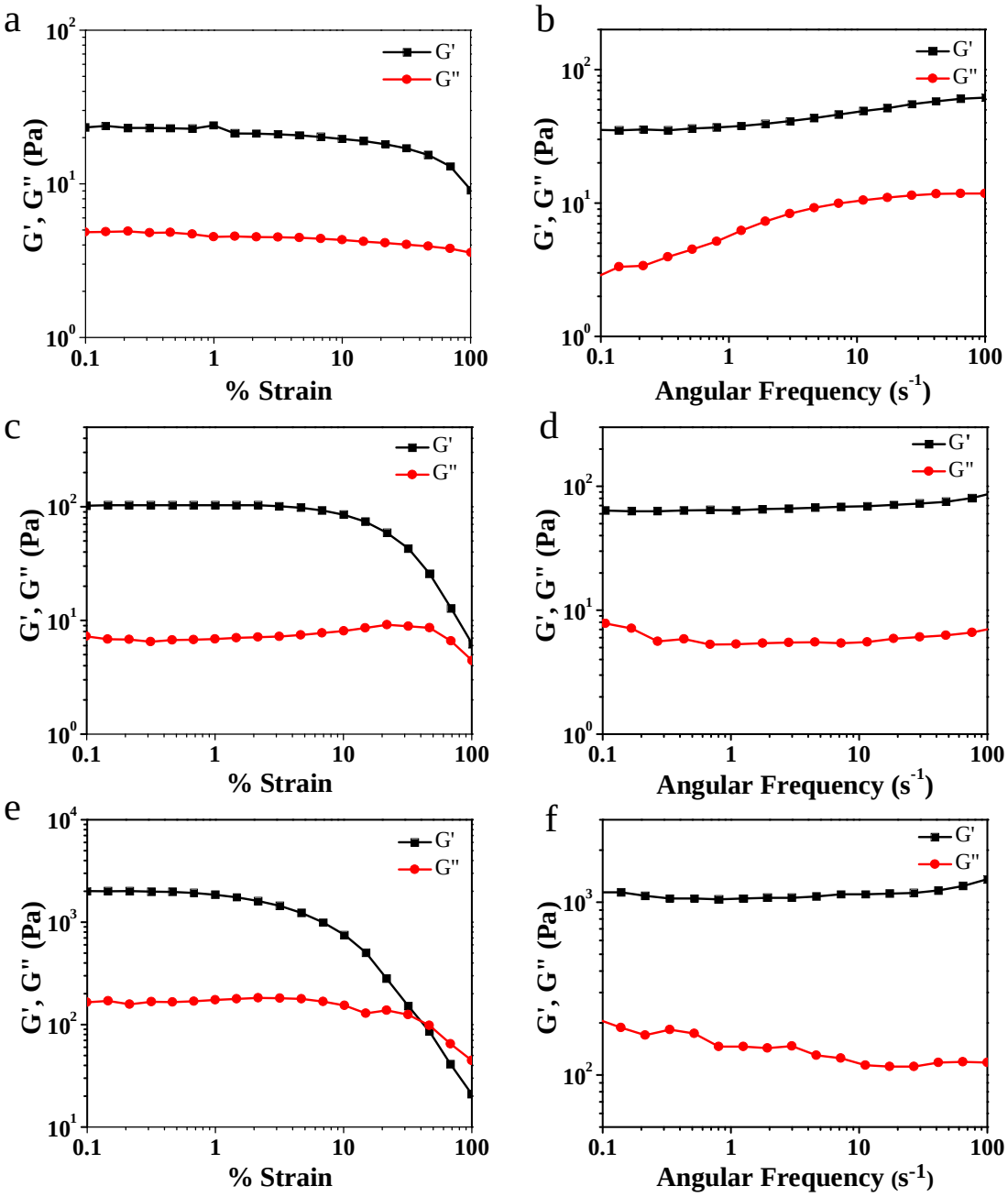

Figure S16. (a), (c) and (e) Amplitude sweep measurement for the Ag-cytosine, Ag-thymine and Ag-uracil gels respectively and (b), (d) and (f) frequency sweep measurement (at a constant strain of 1%) for the Ag-cytosine, Ag-thymine and Ag-uracil gels respectively.

Rheological investigation performed on the three hydrogels suggested that each of the three materials had solid like elastic properties. Both the strain sweep and the frequency sweep experiments were performed and as shown in Fig. S16, for the Ag-cytosine and Ag-thymine gel,

the value of the elastic storage modulus (G′) was greater than the loss modulus (G″) by several factors in both the experiments, indicating the elastic behavior of both the gels. However, in case of Ag-uracil gel, in the strain sweep experiment, it was observed that G′ dominated over G″ upto a strain of 41%, beyond which the material behaved as a viscous sol, as indicated by the higher values of G″ than that of G′. From the values of G′ and G″, it was evident that the Ag-uracil gel was the strongest of the three, whereas the Ag-cytosine gel was the weakest. (G′ for Ag-cytosine, Ag-thymine and Ag-uracil was 0.024 kPa, 0.1 kPa and 2.04 kPa respectively).

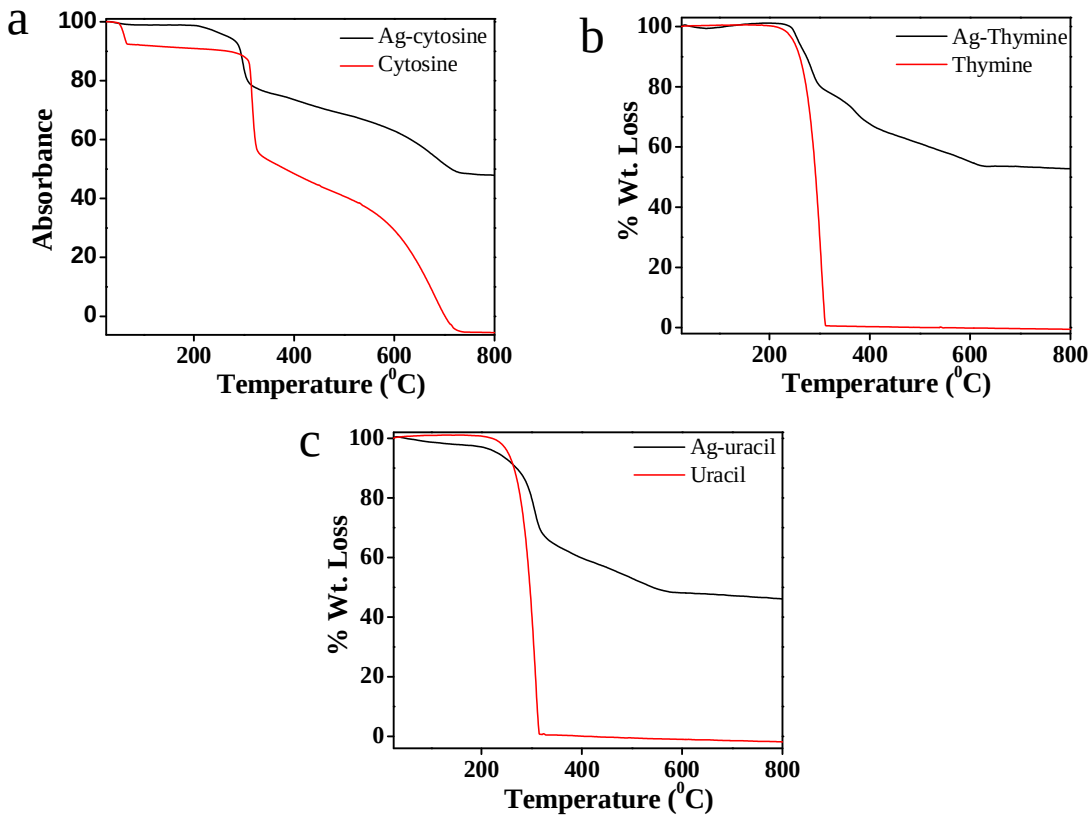

Figure S17. TGA plots of (a) cytosine and Ag-cytosine, (b) thymine and Ag-thymine and (c) uracil and Ag-uracil.

The TGA plot for pure cytosine showed three weight losses at 55 °C, 305 °C and 510 °C resulting in complete decomposition of the organic components. In the TGA plot of Ag-cytosine, similar weight losses were observed. The material however, was stable beyond 720 °C, with a composition of 48%, which might be due to the stability of the metal.

The TGA plot for pure thymine showed a complete decomposition of thymine in a single weight loss in the temperature range of 230 °C-310 °C. For the Ag-thymine xerogels, however a continuous weight loss of 47% was observed in the temperature range of 240 °C-620 °C, suggesting the loss of thymine molecules in this range. Beyond 620 °C, the material was stable as only metallic component was left beyond this temperature.

Similarly, for pure uracil complete decomposition of uracil was observed in a single weight loss in the temperature range of 230 °C-320 °C. On the other hand, for the Ag-uracil xerogels, a continuous weight loss of 52% was observed in the temperature range of 230°C-580°C, which again is attributed to the metallic component (silver) in the Ag-uracil complex.

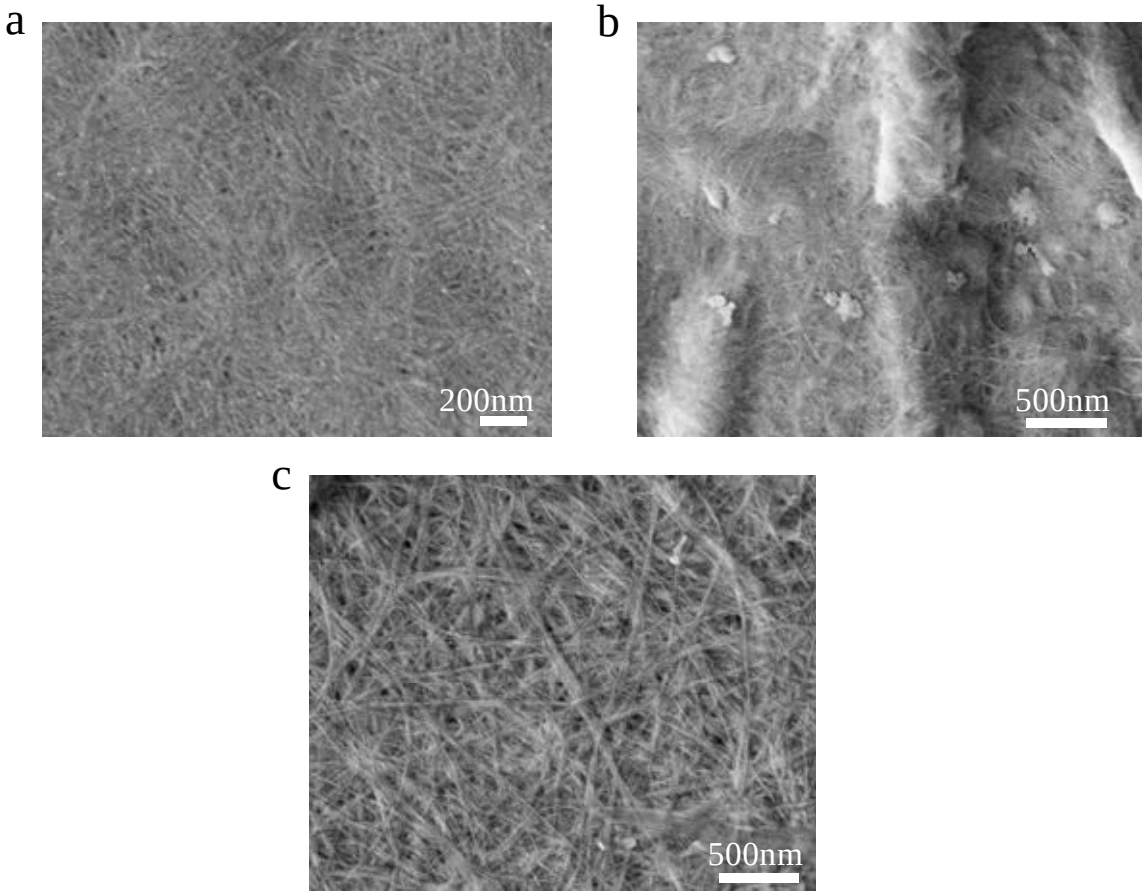

Figure S18. FESEM images of the turbid solution obtained upon the addition of 10 mM $AgNO_3$ to a 10 mM alkaline solution of (a) cytosine, (b) thymine and (c) uracil, showing the formation of fibrous network even at such a low concentration of metal and ligand.

The FESEM images of the turbid solutions of Ag-cytosine, Ag-thymine and Ag-uracil resulting from the addition of low concentration of both Ag^+ ions (10 mM) and nucleobase (8 mM), keeping a metal:base molar ratio of 1:0.8, indicated the formation of fibrous structures as commonly observed in gel materials. The results suggested that the self-assembly process led to the entangled fibrous network even at low concentration. However, for complete entrapment of water in the matrix, higher concentration of Ag^+ ions (100 mM) and nucleobase (80 mM) was required.

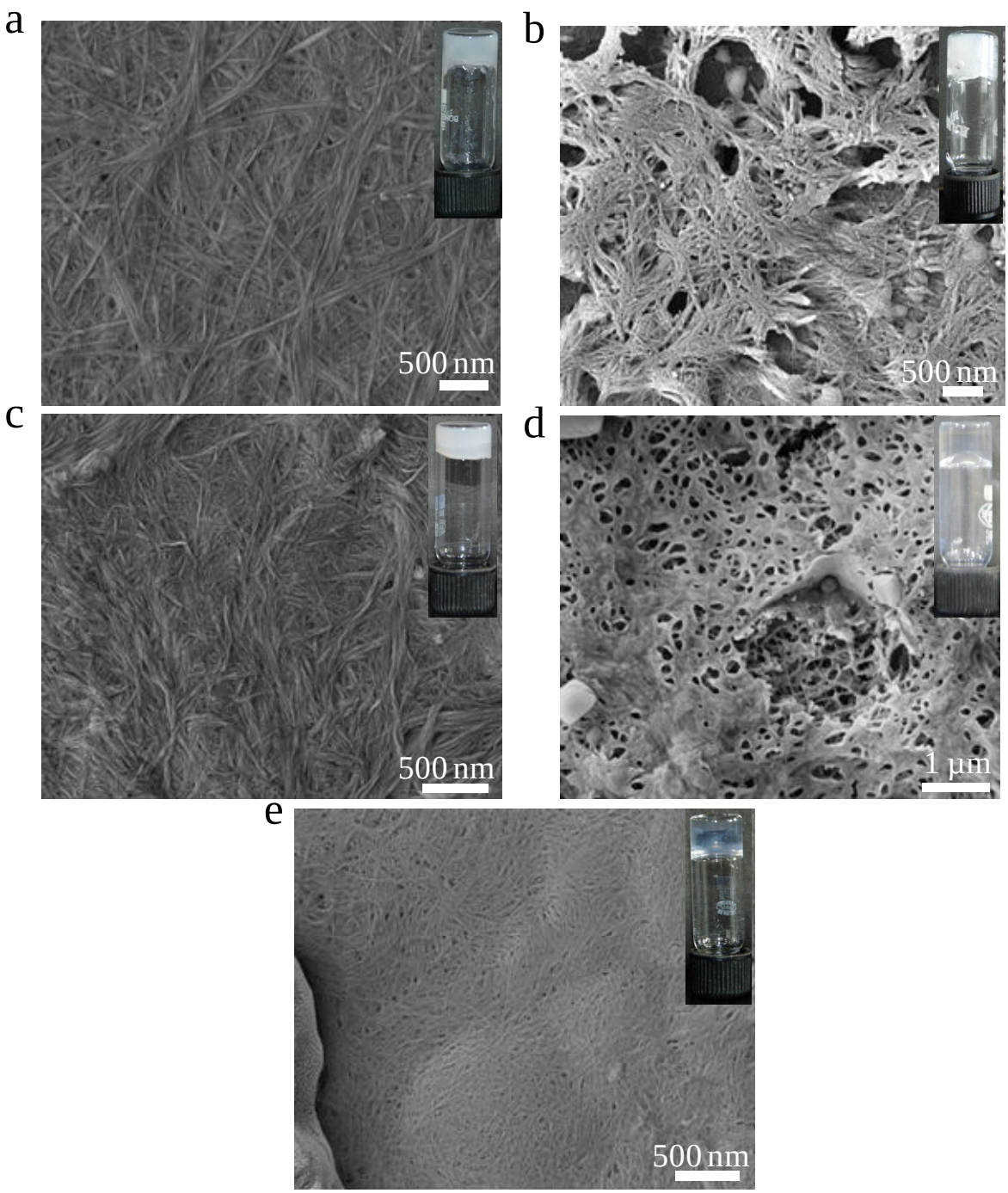

Figure S19. FESEM images of the hydrogels formed upon the interaction of $AgNO_3$ with a mixture of two nucleobases, (a) Ag-adenine-cytosine, (b) Ag-thymine-uracil, (c) Ag-adenine-uracil, (d) Ag-cytosine-thymine, and (e) Ag-cytosine-uracil; *Inset:* Digital images of the respective hydrogels.

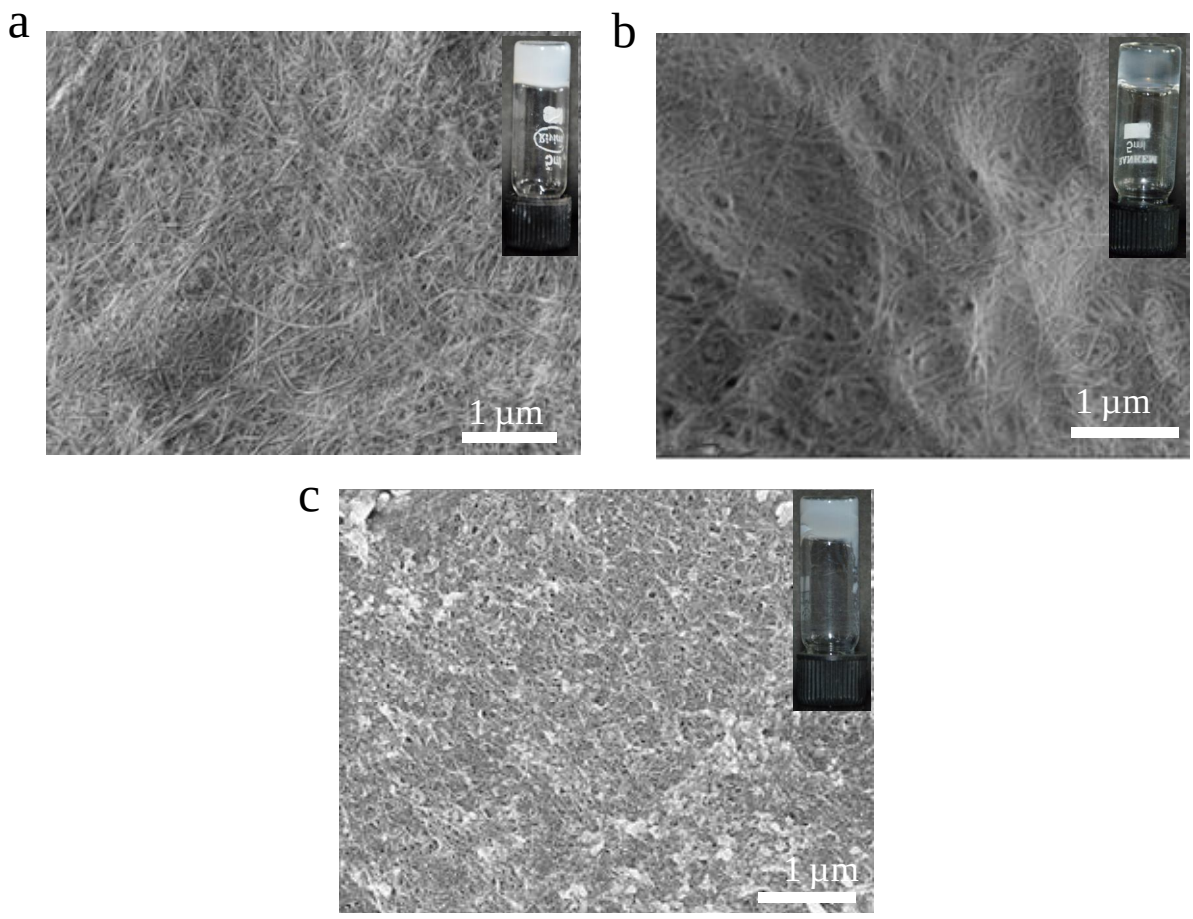

Figure S20. FESEM images of the hydrogels formed upon the interaction of $AgNO_3$ with a mixture of three nucleobases, (a) Ag-adenine-cytosine-uracil, (b) Ag-adenine-thymine- uracil, (c) Ag-cytosine-thymine-uracil and (d) Ag-adenine-cytosine-thymine; *Inset:* Digital images of the respective hydrogels.

From the FESEM images of the hydrogels formed upon the complexation of Ag^+ ions with a mixture of two or three nucleobases, it was very evident that all the hydrogels were composed of three dimensional entangled networks of nanofibers. The water molecules are understandably immobilized within such a nanofibrillar network.

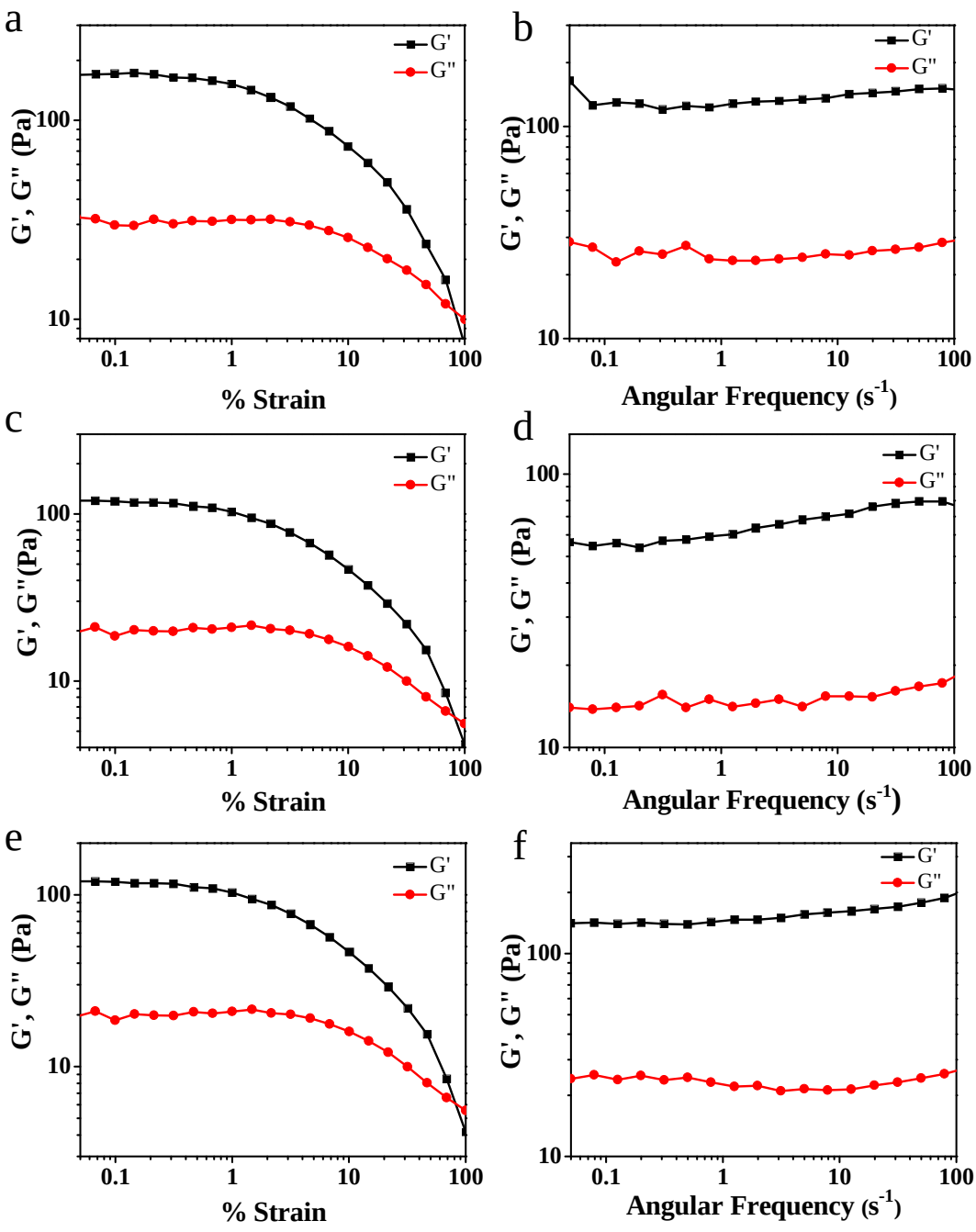

Figure S21. Rheological investigation of hydrogels formed using a mixture of two nucleobases as ligands and Ag^{+} ions as the metallic part. *(*a), (c) and (e) Strain sweep rheological experiment of Ag-adenine-cytosine, Ag-adenine-thymine, and Ag- adenine-uracil gels respectively and (b), (d) and (f) are the frequency sweep experiment at a constant strain of 1% for Ag-adenine-cytosine, Ag-adenine-thymine, and Ag- adenine-uracil gels respectively.

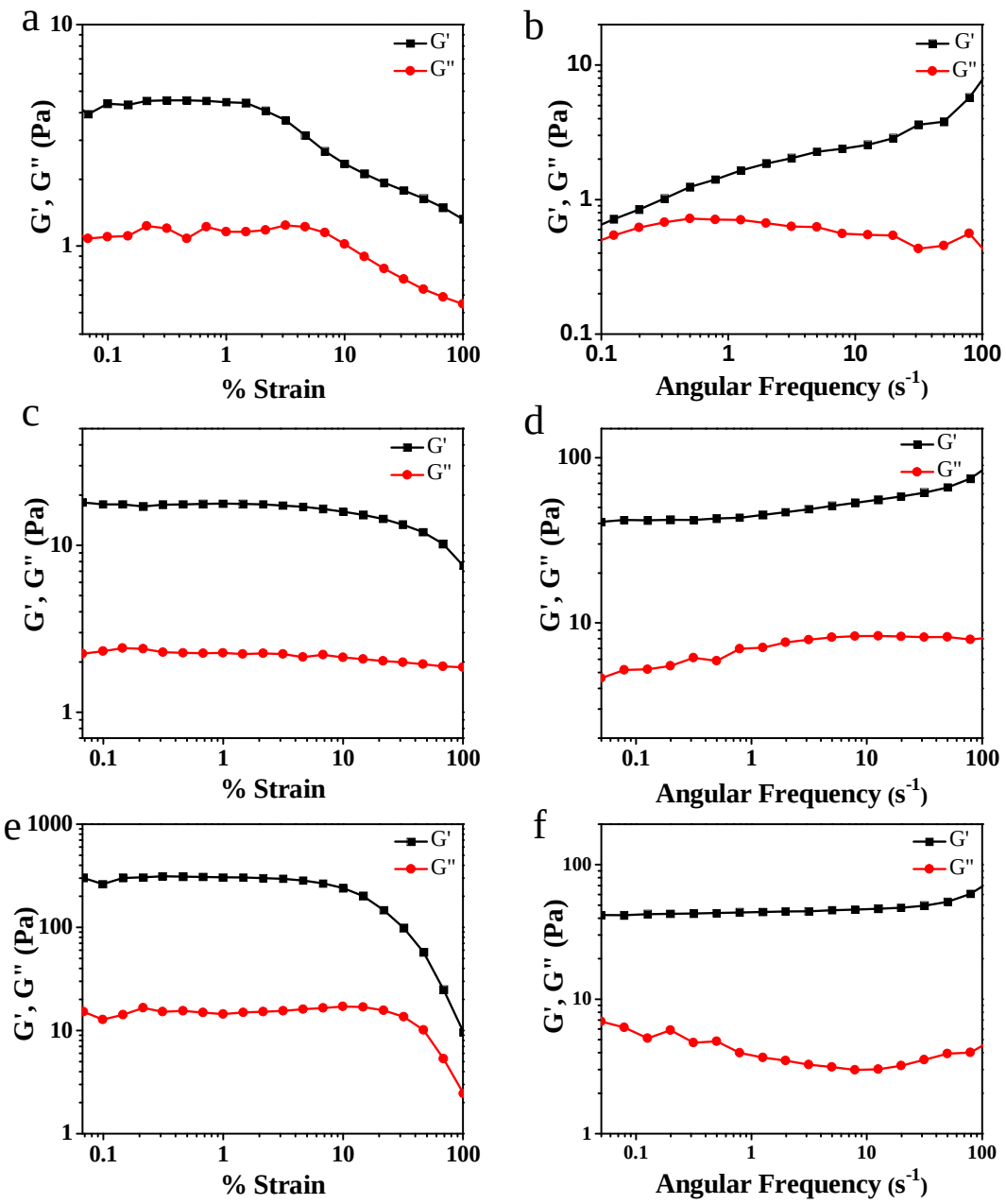

Figure S22. Rheological investigation of hydrogels formed using a mixture of two nucleobases as ligands and Ag^{+} ions as the metallic part. *(*a), (c) and (e) Strain sweep rheological experiment of Ag-cytosine-thymine, Ag-cytosine-uracil and Ag- thymine-uracil gels respectively and (b), (d) and (f) are the frequency sweep experiment at a constant strain of 1% for Ag-cytosine-thymine, Ag-cytosine-uracil and Ag- thymine-uracil hydrogels respectively.

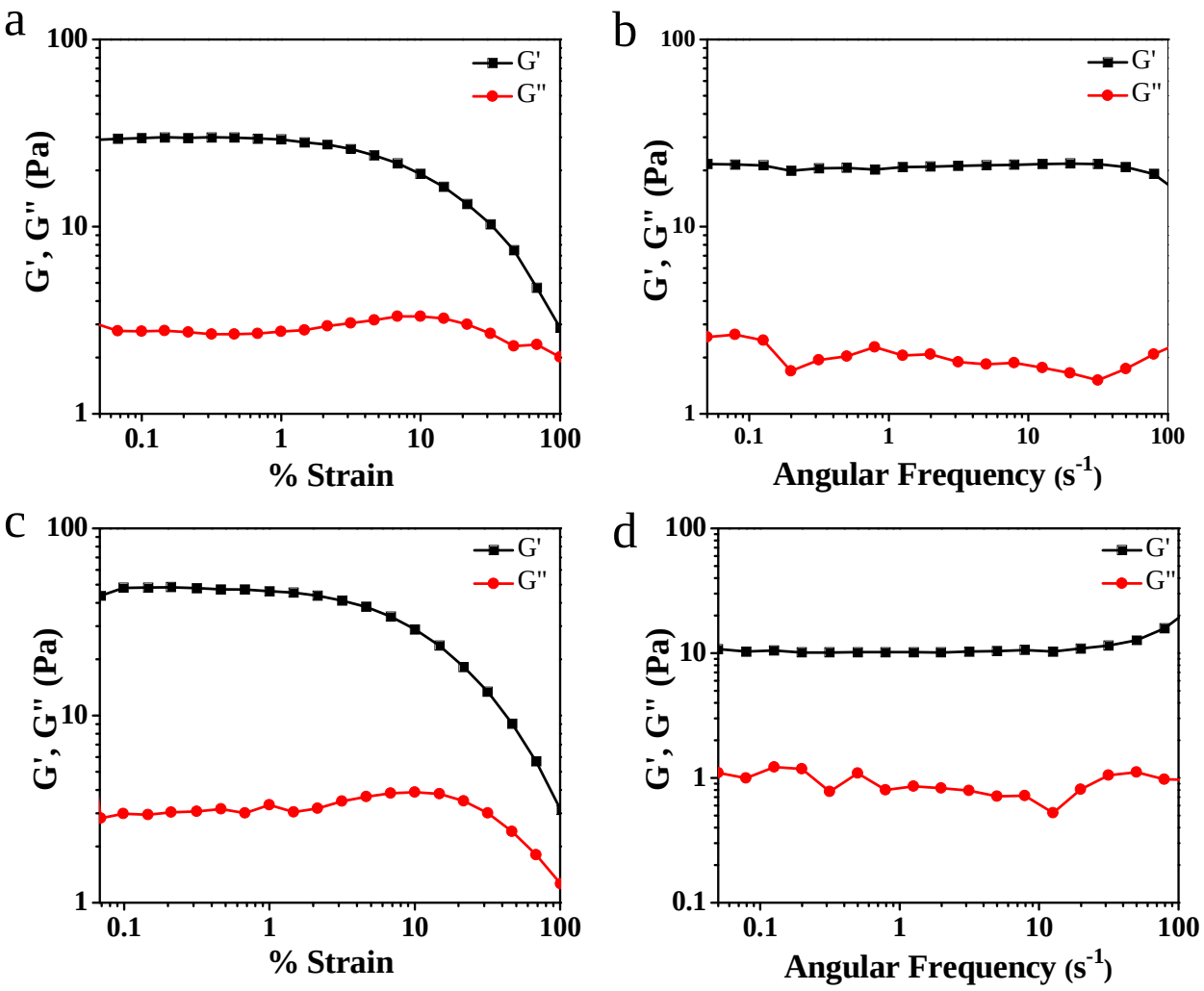

Figure S23. Rheological investigation of hydrogels formed using a mixture of three nucleobases as ligands and Ag^{+} as the metal ions. *(*a), (c) Dynamic strain sweep rheological experiment of Ag-adenine-cytosine-thymine and Ag-adenine-cytosine-uracil gels respectively and (d), (e) are the frequency sweep experiment at a constant strain of 1% Ag-adenine-cytosine-thymine and Ag-adenine-cytosine-uracil hydrogels respectively.

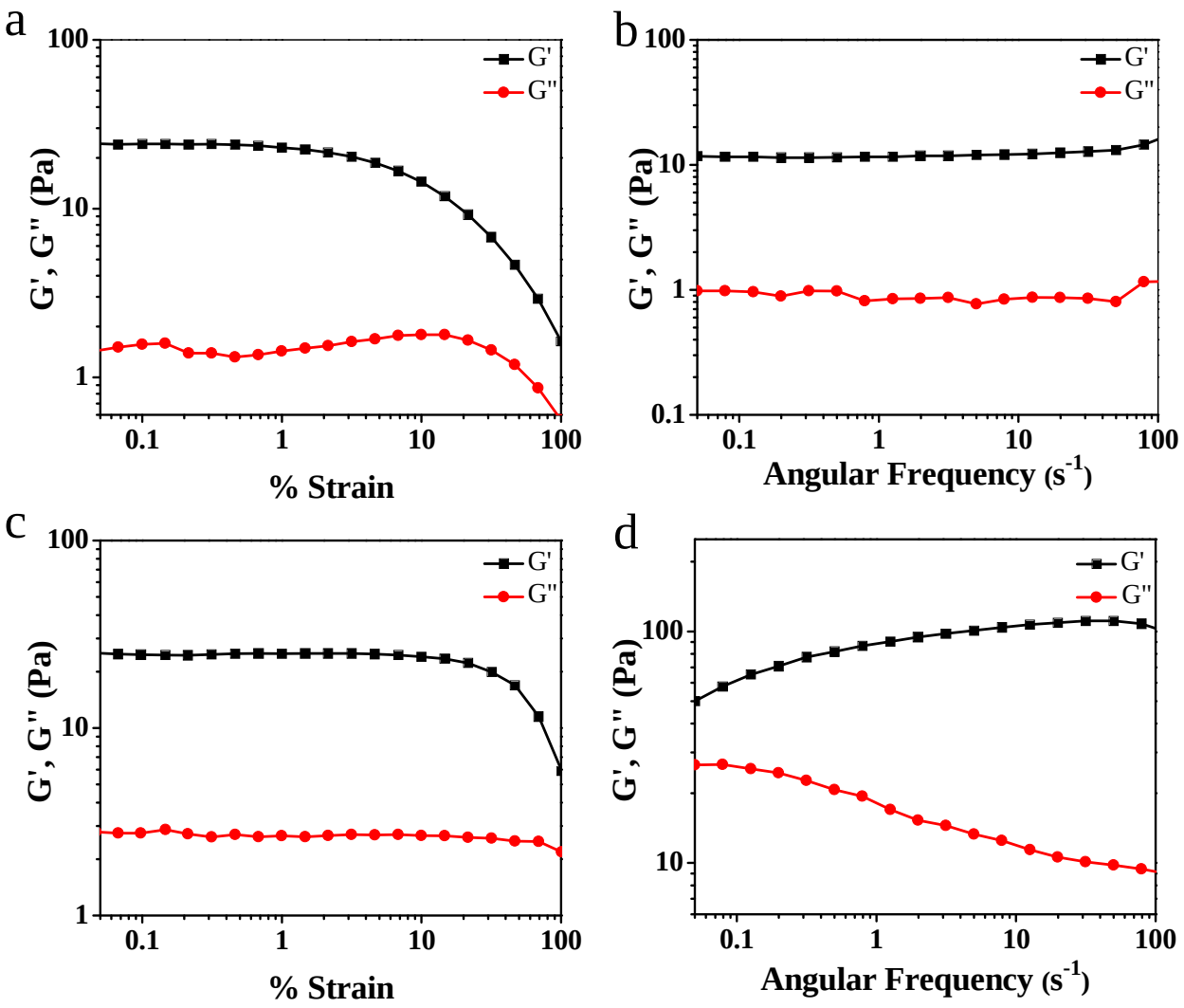

Figure S24. Rheological investigation of hydrogels formed using a mixture of three nucleobases as ligands and Ag^{+} as the metal ions. *(*a), (c) Dynamic strain sweep rheological experiment of Ag-adenine-thymine-uracil and Ag-cytosine-thymine-uracil gels respectively and (d), (e) are the frequency sweep experiment at a constant strain of 1% for Ag-adenine-thymine-uracil and Ag-cytosine-thymine-uracil hydrogels respectively.

From both the dynamic strain sweep and the frequency sweep rheological experiments, it was very evident that all the gels formed using a mixture of two or three nucleobases showed elastic solid like properties as evidenced by the dominance of the storage modulus G′ over the loss modulus G″ in the entire range of strain or frequency.

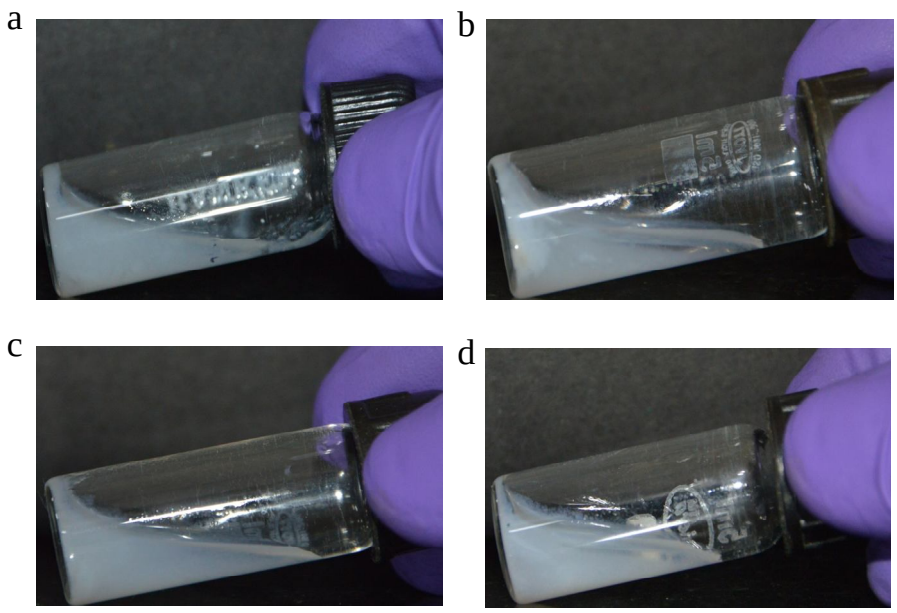

Figure S25. (a) Digital images of the precipitates formed upon the addition of Ag^{+} ions to a mixture of (a) adenine-guanine, (b) cytosine-guanine, (c) thymine-guanine and (d) uracil-guanine.

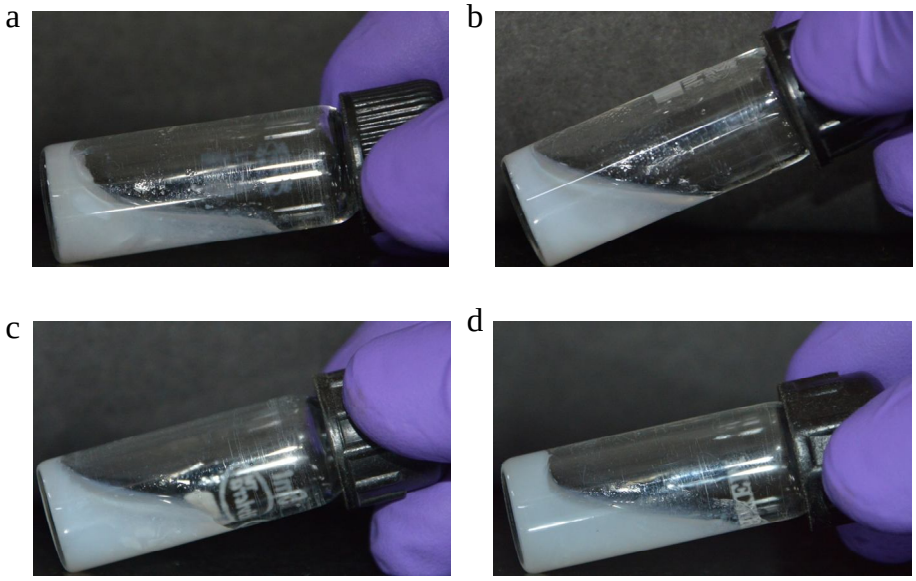

Figure S26. (a) Digital images of the precipitates formed upon the addition of Ag^{+} ions to a mixture of (a) adenine-guanine-uracil, (b) cytosine-guanine-thymine, (c) cytosine-guanine-uracil and (d) thymine-guanine-uracil.

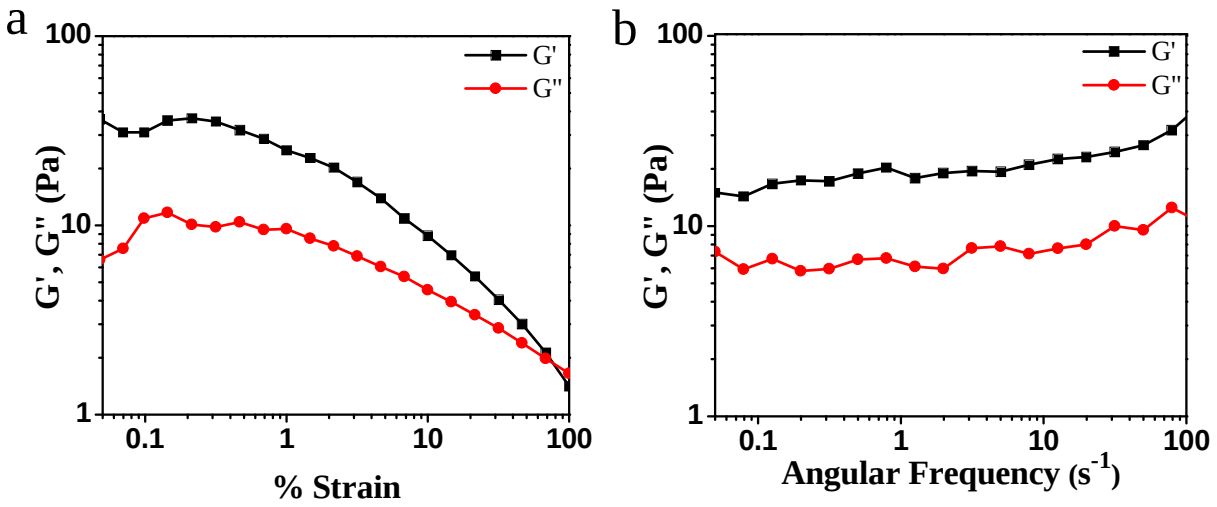

Figure S27. Dynamic strain sweep rheological experiment for Ag-guanine gel formed under acidic conditions and (b) frequency sweep experiment for the Ag-guanine gel formed in acidic medium at a constant strain of 1%.

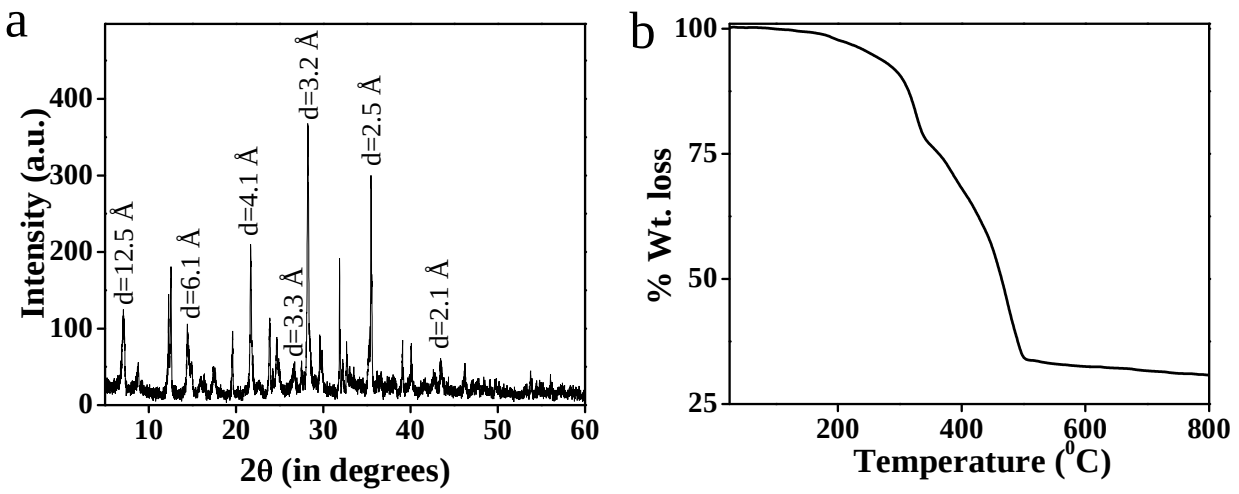

Figure S28. (a) Powder XRD pattern of the lyophilized Ag-guanine gel formed in acidic medium and (b**)** TGA plot for the Ag-guanine gel formed in acidic medium.

The powder XRD spectrum of the lyophilized Ag-guanine gel in acidic medium showed a complex pattern of peaks, suggesting the crystalline nature of the particles formed in the gel (Fig. S28a). From the powder XRD spectrum, major intense peaks at 2θ = 7.1°, 14.4°, 28.3°, 35.5° and 43.5° corresponding to *d*- spacing of 12.5 Å, 6.1 Å, 4.1 Å, 3.2 Å and 2.1 Å respectively were observed in addition to several other sharp peaks. These peaks followed a ratio of 1: 1/2: 1/3: 1/4: 1/5, suggesting that the hydrogels were mainly assembled in a layered structure and the interlayer distance was 12.5 Å. Along with these peaks, a broad peak at 2θ = 26.7° was observed, which corresponded to a *d*- value of 3.3 Å that could be related to the π-π stacking interactions between two adjacent guanine molecules[7]. Thermogravimetric analysis of the lyophilized gel was performed to study the thermal stability of the gel. From the TGA plot, two weight losses with a total mass loss of 66% in the temperature range of 180-500 °C were observed (Fig. S28b). This could be attributed to the decomposition of the ligands (guanine) in the Ag-G complex.

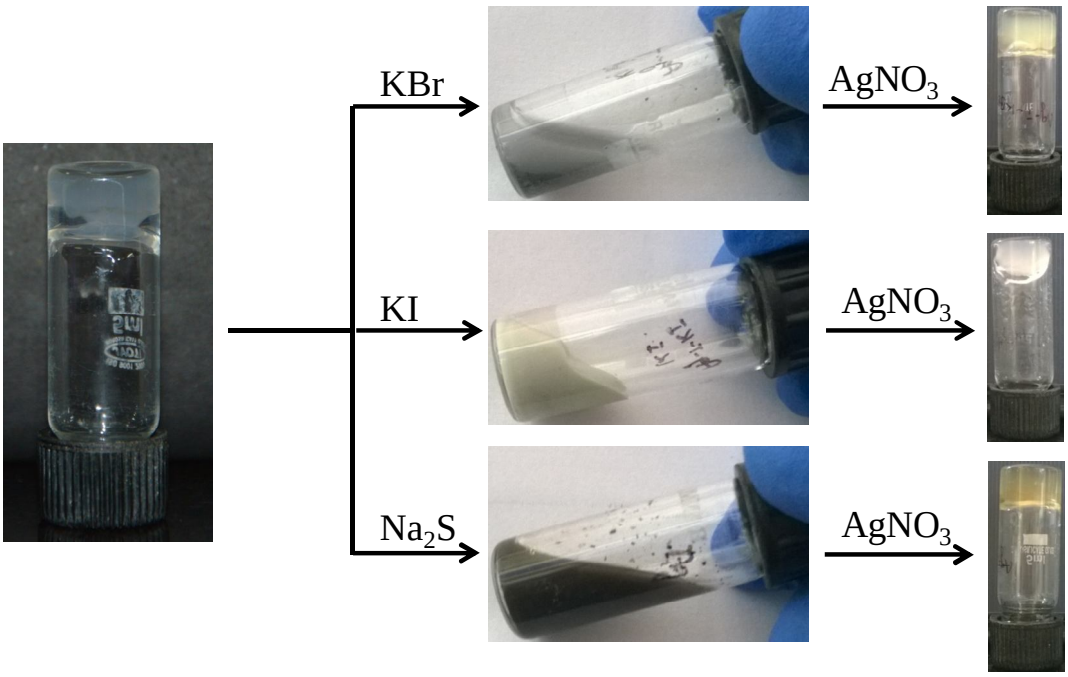

Figure S29. Schematic illustration of the chemical response of the Ag- nucleobase gels towards different chemicals. All these examples are shown with the Ag-thymine gel.

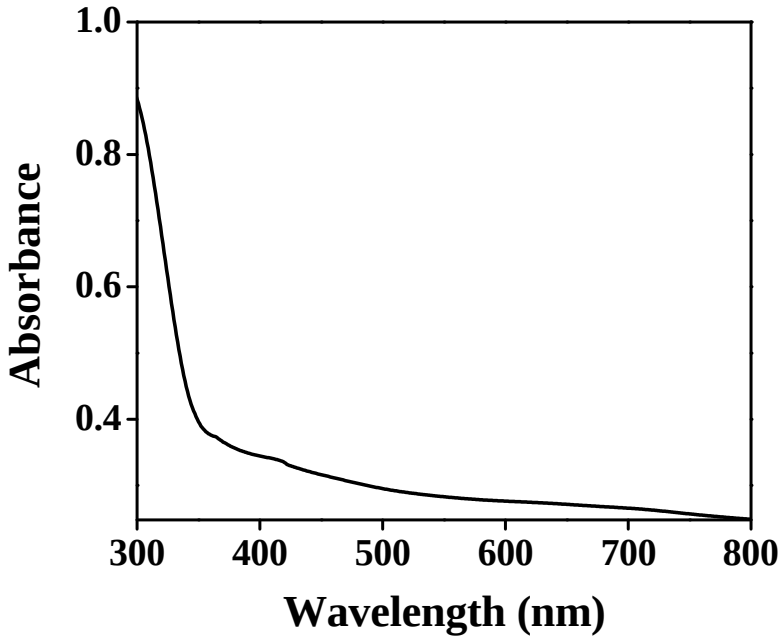

Figure S30. Solid state UV-visible spectrum of Ag-adenine gel showing the absence of the characteristic SPR band of Ag nanoparticles.

DFT studies

Basic Medium

As single crystals suitable for X-ray diffraction studies could not be obtained, therefore, to have an idea on the nature of bonding in the hydrogels, density functional theory (DFT) studies were carried out. Under the basic condition, we assume that the most acidic hydrogen (with lowest pKa) are deprotonated from the nucleobases.[8-10] Here, N9-H, N1-H, N1-H, N3-H and N3-H are the most acidic hydrogen for adenine, guanine, cytosine, uracil, and thymine, respectively. It is well known that counter anions play a vital role in the formation of polymeric networks such as metallogels. Therefore, we calculated the binding energy between the silver and nitrate in its pure form and upon binding to nucleobases. It is clear from Table S3 that binding energy of silver with nucleobase is not affected much, when it binds to the nucleobases along with nitrate, indicating that nitrate ions have a negligible influence on the binding of silver to the nucleobases. So, it must be the binding of silver ions to the nucleobases and the hydrogen bonding, which is responsible for the formation of the hydrogels.

System	Adenine		Cytosine		Thymine		Uracil		Guanine	
	Basic	Acidic	Basic	Acidic	Basic	Acidic	Basic	Acidic	Basic	Acidic
NO3Ag----Nucleo	-22.45	-15.34	-24.06	-9.85	-25.32	-	-24.99	-	-23.45	-20.80
Ag---Nucleo	-21.47	-	-23.59	-	-24.23	-	-24.66	-	-24.33	-
NucleoAg----NO3	-15.21	-16.53	-14.74	-15.47	-14.87	-	-14.87	-	-13.35	-14.78
Ag----NO3 (pure)	-14.19									

Table S3. Binding energy of (1) silver with nucleobases (first two rows) with and without nitrate, (2) silver with nitrate (last two rows) when bound to nucleobases and the binding energy of pure $AgNO_3$.

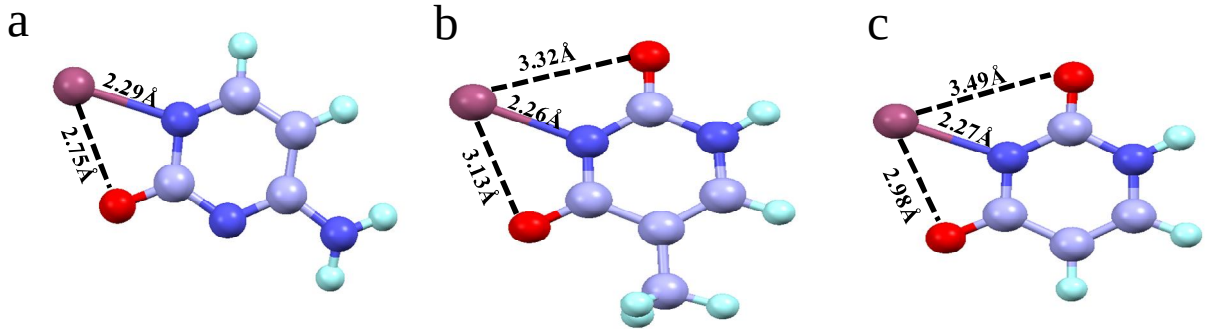

Figure S31. Optimized structure of silver-nucleobase monomeric unit in basic medium. [(a) Ag-cytosine, (b) Ag-thymine and (c) Ag-uracil hydrogels].

To explore the polymeric nature of these silver-nucleobase units, we considered two metal-nucleobase units. Different binding sites and different orientations of the second nucleobase-silver unit are considered to bind with the previous unit and the most energetically stable structure is considered as the nucleobase-silver dimeric unit. The most preferred nucleobase-silver dimeric unit for the three pyrimidine nucleobases is shown in figure S32. As clearly indicated in the figure, all the three pyrimidine units, together with adenine units (Fig. 4c; main text) can be extended further to give polymeric chains and this result in the formation of hydrogels when adenine, cytosine, thymine and uracil are used as ligands.

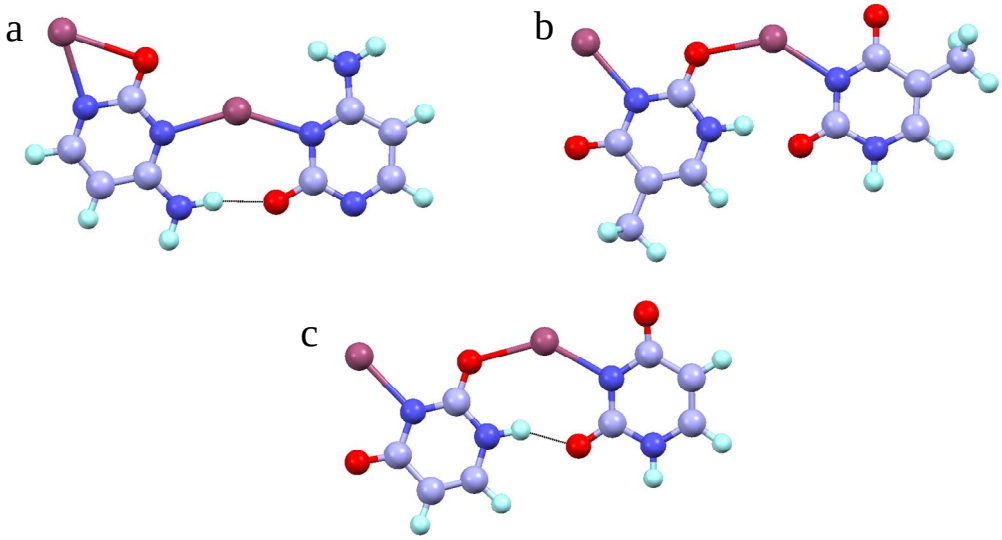

Figure S32. Optimized structure of silver-nucleobase dimeric unit in basic medium. [(a) Ag-cytosine, (b) Ag-thymine and (c) Ag-uracil hydrogels].

Acidic Medium

Under acidic conditions, protonation occurs at that specific site of the nucleobase which shows highest pKa values among all possible sites. Accordingly, N1, N3 and N3 are the most preferred sites for protonation of adenine, guanine and cytosine respectively. Uracil and thymine have extremely low pKa values, suggesting their reluctance to protonation. Literature reports have shown that at acidic pH, the metal counter ions largely facilitate the formation of a crystal upon the interaction of the metal salts with the nucleobases.[11,12] The calculated binding energies (Table S3) show that nitrate ions bind strongly to the silver when silver is bonded to nucleobase unit which implies that binding of nitrate to the silver atom is the main driving force for the silver-nucleobase bonding. In case of adenine, binding of silver and nitrate is very strong (-16.53 kcal/mol) which suggest that positive charge of silver is compensated by nitrate. This prevents silver to bind to another nucleobase unit for the formation of polymeric chain, resulting in the precipitation of monomeric silver-nucleobase unit. In contrast, binding of silver with guanine is very (-20.80 kcal/mol) strong than the binding of silver and nitrate (-14.78 kcal/mol) in case of guanine. It implies that Ag-guanine binding is more favorable than Ag-NO_3 binding, which helps in the formation of polymeric chain. Besides, O-sites are free for hydrogen bonding with water, helping to the formation of hydrogel. In case of cytosine, silver-nucleobase binding (-9.85 kcal/mol) is not favorable, since silver-nitrate binding is relatively strong (-15.47 kcal/mol), suggesting its tendency to remain as $AgNO_3$. The theoretical prediction agrees well with experimental results where a clear solution was obtained in case of cytosine which might be due to the $AgNO_3$ solution. Due to the significantly lower binding energy of silver and cytosine, thymine or uracil, silver nitrate remained as such, resulting in a clear solution. The optimized structures of silver-nucleobase monomeric units under acidic conditions are shown in Fig. S33.

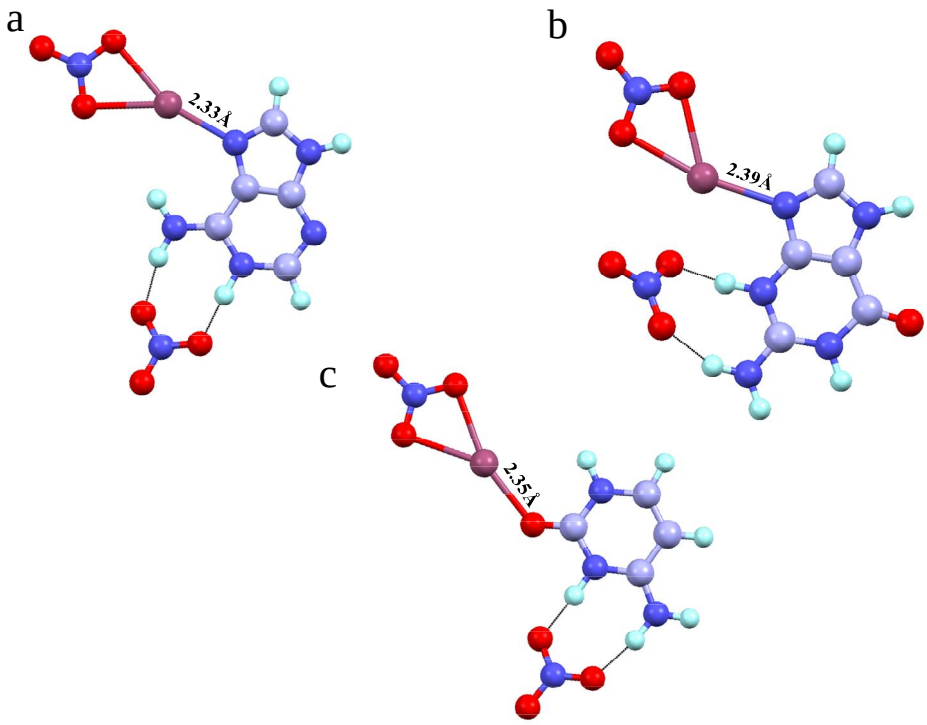

Figure S33. Optimized structure of silver-nucleobase monomeric unit in acidic medium. [(a) Ag-adenine, (b) Ag-guanine and (c) Ag-cytosine].

To explore the polymeric nature of these silver-nucleobase units in acidic medium, we considered two metal-nucleobase units. Different binding sites and different orientations of the second nucleobase-silver unit were considered to bind with the previous unit and the energetically most stable structure was considered as the nucleobase-silver dimeric unit. The most preferred nucleobase-silver dimeric unit for the three nucleobases, based on the DFT studies is shown in the Fig. S34.

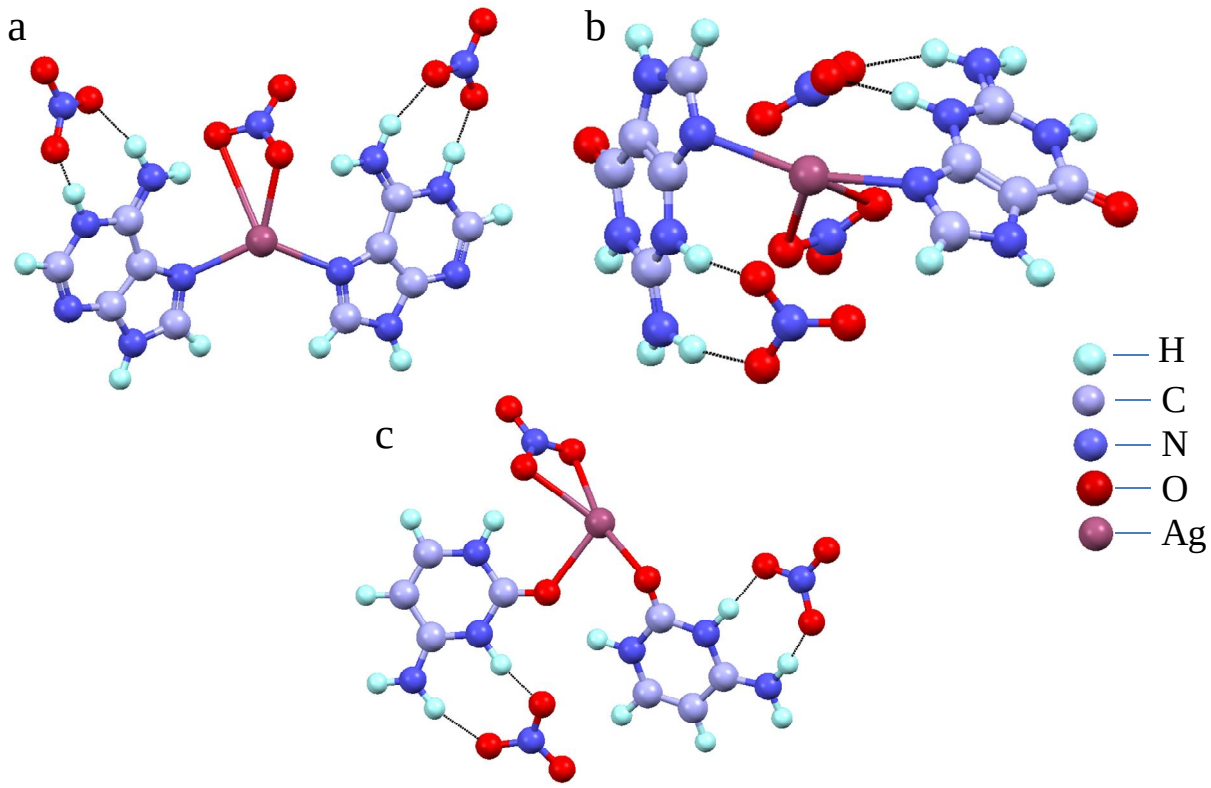

Figure S34. Optimized structure of silver-nucleobase dimeric unit in acidic medium. [(a) Ag-adenine, (b) Ag-guanine and (c) Ag-cytosine].

Microbe	Hydrogel	Volume of gel (μL)	Diameter of zone of inhibition (mm)
E. coli	Ag-adenine	10	10
		20	10
		30	11
		40	12
	Ag-cytosine	10	11
		20	12
		30	13
		40	14
	Ag-thymine	10	13
		20	13
		30	14
		40	15
	Ag-uracil	10	15
		20	16
		30	17
		40	18

Table S4. Effect of amount of hydrogel on the antimicrobial activity of the Ag-nucleobase hydrogels against *E.coli* bacterium.

Microbe	Hydrogel	Volume of gel (μL)	Diameter of zone of inhibition (mm)
S.aureus	Ag-adenine	10	11
		20	12
		30	12
		40	13
	Ag-cytosine	10	14
		20	15
		30	16
		40	17
	Ag-thymine	10	15
		20	16
		30	17
		40	18
	Ag-uracil	10	19
		20	20
		30	21
		40	21

Table S5. Effect of amount of hydrogel on the antimicrobial activity of the Ag-nucleobase hydrogels against *S. aureus* bacterium.

References

1. M. J. Frisch, G. W. Trucks, H. B. Schlegel, G. E. Scuseria, M. A. Robb, J. R. Cheeseman, G. Scalmani, V. Barone, B. Mennucci, G. A. Petersson, H. Nakatsuji, M. Caricato, X. Li, H. P. Hratchian, A. F. Izmaylov, J. Bloino, G. Zheng, J. L. Sonnenberg, M. Hada, M. Ehara, K. Toyota, R. Fukuda, J. Hasegawa, M. Ishida, T. Nakajima, Y. Honda, O. Kitao, H. Nakai, T. Vreven, J. A. Montgomery, Jr., J. E. Peralta, F. Ogliaro, M. Bearpark, J. J. Heyd, E. Brothers, K. N. Kudin, V. N. Staroverov, R. Kobayashi, J. Normand, K. Raghavachari, A. Rendell, J. C. Burant, S. S. Iyengar, J. Tomasi, M. Cossi, N. Rega, J. M. Millam, M. Klene, J. E. Knox, J. B. Cross, V. Bakken, C. Adamo, J. Jaramillo, R. Gomperts, R. E. Stratmann, O. Yazyev, A. J. Austin, R. Cammi, C. Pomelli, J. W. Ochterski, R. L. Martin, K. Morokuma, V. G. Zakrzewski, G. A. Voth, P. Salvador, J. J. Dannenberg, S. Dapprich, A. D. Daniels, Ö. Farkas, J. B. Foresman, J. V. Ortiz, J. Cioslowski, D. J. Fox. **2009**, Gaussian 09, Revision A.1, Gaussian Inc., Wallingford CT
2. Y. Zhao, D. G. Truhlar, *Acc. Chem. Res.*, 2008, **41**, 157.
3. J. Tomasi, M. Persico, *Chem. Rev*., 1994**, 94**, 2027.
4. M. Cossi, V. Barone, R. Cammi, J. Tomasi, *Chem. Phys. Lett*., 1996, **255**, 327.
5. V. Barone, M. Cossi, J. Tomasi, *J. Chem. Phys*., 1997, **107**, 3210.
6. V. Barone, M. Cossi, J. Tomasi, *J. Comput. Chem*., 1998, **19**, 404.
7. R. N. Das, Y. P. Kumar, S. Pagoti, A. J. Patil, J. Dash, *Chem.- Eur. J.*, 2012, **18**, 6008...
8. V. Verdolino, R. Cammi, H. Munk, H. B. Schlegel, *J. Phys. Chem. B*, 2008, **112**, 16860.
9. B. Lippert, D. Gupta, *Dalton Trans.*, 2009, 4619.
10. Y. H. Jang, L. C. Sowers, T. Cagin, W. A. Goddard III, *J. Phys. Chem. A*, 2001, **105**, 274.
11. C. S. Purohit, A. K. Mishra, S. Verma, *Inorg. Chem.*, 2007, **6**, 8493.
12. K. D. Klika, H. Kivelä, V. V. Ovcharenko, V. Nieminen, R. Silanpää, J. Arpalahti, *Dalton Trans.*, 2007, **21**, 3966.